ENTATION PAGE

Form Approved
OMB No. 0704-0188

1. AGENCY USE ONLY (Leave blank)	2. REPORT DATE	3. REPORT TYPE AND DATES COVERED
	August 1994	Scientific Paper

4. TITLE AND SUBTITLE

ISSSR Tutorial 1: Introduction to Spectral Remote Sensing

5. FUNDING NUMBERS

6. AUTHOR(S)

Dr. John Rinker

7. PERFORMING ORGANIZATION NAME(S) AND ADDRESS(ES)

U.S. Army Topographic Engineering Center
ATTN: CETEC-PAO
7701 Telegraph Road
Alexandria, VA 22315-3864

8. PERFORMING ORGANIZATION REPORT NUMBER

R-238

9. SPONSORING/MONITORING AGENCY NAME(S) AND ADDRESS(ES)

10. SPONSORING/MONITORING AGENCY REPORT NUMBER

11. SUPPLEMENTARY NOTES

12a. DISTRIBUTION/AVAILABILITY STATEMENT

Approved for public release;
distribution is unlimited.

13. ABSTRACT *(Maximum 200 words)*

This tutorial, the first of a linked set of four, provides an introduction to remote sensing as a tool for studying the earth, its land, water bodies, cultural components, and surrounding atmosphere. The basis for this capability is the recording of reflected, emitted, and luminesced photons, usually in the form of images, and the subsequent interpretation of image patterns for terrain information (manual analysis), and of spectral patterns for targeting, monitoring, and change detection (computer and digital analysis). Included are brief reviews of: radiation characteristics such as bandwidth, interference, absorption, reflectance, emittance, luminescence; optical attributes such as focus, and resolution; research results in spectral measurements; and application examples from various remote sensing systems. This leads to Tutorial II on spectral measurements; thence to Tutorial III on the digital analysis of imaging spectrometer data; and to Tutorial IV on the characteristics of available remote sensing systems.

14. SUBJECT TERMS	15. NUMBER OF PAGES
spectral measurements, remote sensing, multiband, hyperspectral, image analysis	39
	16. PRICE CODE

17. SECURITY CLASSIFICATION OF REPORT	18. SECURITY CLASSIFICATION OF THIS PAGE	19. SECURITY CLASSIFICATION OF ABSTRACT	20. LIMITATION OF ABSTRACT
unclassified	unclassified	unclassified	

image Analysis

ISSSR TUTORIAL I[1]
INTRODUCTION TO SPECTRAL REMOTE SENSING

J. N. Rinker
U. S. Army Topographic Engineering Center
Alexandria, Virginia 22315-3864, USA

ABSTRACT

This tutorial, the first of a linked set of four, provides an introduction to remote sensing as a tool for studying the earth, its land, water bodies, cultural components, and surrounding atmosphere. The basis for this capability is the recording of reflected, emitted, and luminesced photons, usually in the form of images, and the subsequent interpretation of image patterns for terrain information (manual analysis), and of spectral patterns for targeting, monitoring, and change detection (computer and digital analysis). Included are brief reviews of: radiation characteristics such as bandwidth, interference, absorption, reflectance, emittance, luminescence; optical attributes such as focus, and resolution; research results in spectral measurements; and application examples from various remote sensing systems. This leads to Tutorial II on spectral measurements; thence to Tutorial III on the digital analysis of imaging spectrometer data; and to Tutorial IV on the characteristics of available remote sensing systems.

1. INTRODUCTION

Remote sensing systems rely on a variety of energy forms such as pressure waves, or sonar (sound navigation and ranging), gravity, radio activity, and electrical and magnetic fields. The workhorse, however, is electromagnetic radiation; reflected, emitted, or luminesced. Such radiation comes from natural sources, such as the sun, from man-made sources such as flashbombs, lasers (light amplification by stimulated emission of radiation), or radio antennae as in radar (radio detection and ranging). How it is measured is of equal diversity and includes sensors such as the eye, photographic emulsions, photo cells, antennae, charge coupled devices, thermistors, etc. Most often, the results are presented as an image, or an assemblage of images, wherein each image portrays the terrain in a different band of the electromagnetic spectrum, e.g., multiband, multispectral, or hyperspectral.

Why the interest in multiband and hyperspectral remote sensing?—simply because these techniques provide more information. Materials respond differently in different parts of the electromagnetic spectrum. An image recorded in one band can depict patterns not discernable in images recorded in other bands. To illustrate this, Fig. 1 shows images of human torsos recorded with: A, reflected visible (400-700 nm); B, reflected near-infrared (700-800 nm); C, emitted thermal infrared (800-1400 nm); and D, transmitted x-ray radiation (0.1 nm range). In all cases, however, identification of the various features relied on shape patterns and their location. The visible light photograph (A) shows surface characteristics of the skin cover of the torso. That it is a torso is verified by its shape. The identification of the nipples also relies on shape patterns and locations. Near-infrared radiation (image B), having longer wavelengths, penetrates further into the skin and records subsurface differences in absorption; as evident in the interconnected pattern of dark lines, whose shape, size, and location identifies it as part of the vascular system. In the thermal infrared image (C), brightness differences result from temperature variations on the skin surface. The bright irregular pattern is caused by a tumor, the cells of which have a higher metabolic rate, and thus a higher temperature than normal

[1]This tutorial is based on earlier publications (Rinker, 1990a and b), and the Tutorial for ISSSR 1992.

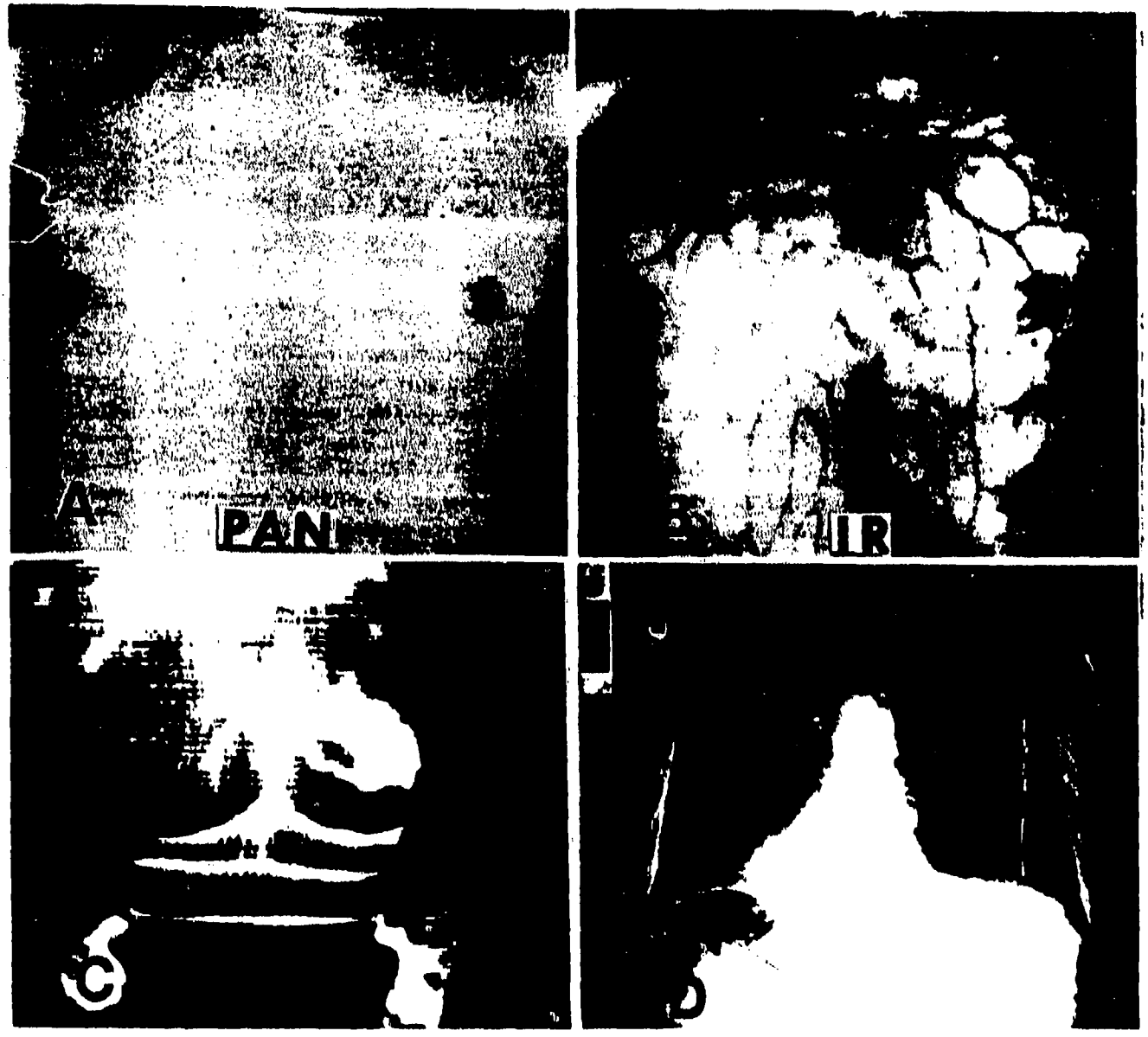

Figure 1. Human torsos as viewed in different spectral bands. Image A, a visible light record, shows only surface details of the skin, e.g., the pattern of the nipples, identifiable by shape and location. Image B was formed with reflected infrared energy, which penetrated the skin to depict the underlying vascular structure, identifiable by its shape and location. These images (A and B) are from an old Eastman Kodak Manual. Image C (Wallace, 1974 personal communication) is a record of thermal infrared energy wherein the brightness of tone is related to temperature. The bright irregular pattern on the breast results from a tumor. A tumor has a higher metabolic rate, and a slightly higher temperature than its surrounds. By conduction, it has warmed the skin over it and revealed its presence. The spectral band records it as a warmer object; the shape and location of the thermal pattern provides the identity. The bright linear patterns below the tumor represent warmer temperatures associated with folds in the skin. Image D, an x-ray record, shows internal structures within a torso, identifiable by their shapes and locations, as ribs, clavicle, joint, etc.

cells. By conduction, the tumor has made the skin over it warmer than the skin adjacent—revealing its presence. It is the shape and location of the thermal pattern, however, that suggest the presence of a tumor.

The shapes and locations of other equally light-toned, and warm areas, are indicative of folds in the skin. In the x-ray image (D), the brightness variations are caused by differences in tissue density through which the x-rays passed. But, it is the shapes and locations of the image patterns that provide identification, e.g., ribs, clavicle, sternum, etc.

Figure 2 is an example from the satellite remote sensing domain. The left image is a Landsat scene of a portion of the North African desert, showing only the surface patterns of the terrain. To the right is the same image, but with a superposed strip from the Shuttle Imaging Radar (SIR-A) imagery of the same area. The L-band microwave energy penetrated the surface deposits of sand and gravel to reveal an underlying pattern of an ancient drainage system (McCauley, 1982). The radar band provided the means for recording the details, and the shapes of the pattern elements provided identification. If one had but the radar image, would the conclusion arise that it was a buried drainage system? Radar does record surface drainage patterns. Band comparison can be as critical to the derivation of information, as can the contents within bands.

Because all materials reflect, absorb, or emit photons in ways characteristic of their molecular makeup, a high-resolution trace of the intensity of the transmitted, reflected, emitted, or luminesced radiation versus wavelength forms a graphical record unique to a given material. Different materials cannot have identical spectral wave shapes of reflectance, emittance, and luminescence. Many of the characteristic absorption and emission bands occur in narrow wavelength ranges, 10 nm or less; and, unless the instruments have that kind of spectral resolution, these details cannot be recorded. Although many laboratory and field instruments exceed this spectral resolution, airborne systems have only recently entered this domain. From a laboratory point of view, the use of spectral measurements to identify and/or assay components of minerals, pigments, pharmaceutical and other organic and inorganic compounds, is old, established, and reliable. The reasoning goes that if such could be done from air or space, it would give remote sensing a similar capability.

Figure 2. The left image is a Landsat MSS scene over North Africa. To the right, an L-band radar image (SIR-A) is registered over the scene. The radar penetrated the surface deposits, to reveal a buried drainage system from an earlier time (McCauley, 1982).

1.1 TERRAIN ANALYSIS

Reliable, detailed information about the landscape in terms of composition, structure, properties, conditions, and use is fundamental to predicting terrain characteristics, be it for engineering site selection and evaluation, environmental impact studies, or military operations such as cross-country movement. Foremost to these applications, but more intuitively apparent in relation to cross-country movement, are questions such as: is it flat?—is it rolling?—is it a hill?—is it steep?—are the slopes smooth, stepped (thinly bedded, or massively bedded)?—is the surface dissected (drainageways as indicators of composition, as obstacles, as ambush sites, or for cover and concealment)?—are the channel slopes steep, or gentle? These questions involve shape, and for this purpose stereo imagery is the only source of accurate information. For example, an area can be covered with a vegetative mantle of grass and trees, and all that the spectral data will show will be reflectance traces of chlorophyll. In stereoscopic viewing, however, the shapes of the landform and drainage patterns can reveal that beneath the vegetal mantle rests a thinly interbedded series of gently dipping limestones and shales with unstable colluvial materials on the lower slopes.

Three-dimensional shapes are directly related to the composition, structure, physical properties, conditions and climatic regime of the resident materials, and thereby serve as indicators of these factors. Patterns in an image can be classified into landform, drainage (plan and elevation, i.e., cross section and gradient), erosion, deposition, vegetation, tone and texture, cultural, and "special," which includes such features as joints, faults, slumps, tears, mud flows, trim lines, etc. Topographic shape, i.e., landform, identifies landscape elements as plains, valleys, hills, mountains, escarpments, fans, terraces, etc., and their specific shapes provide clues about composition and physical properties. The shapes of the drainageways, in plan and elevation, convey information about soil type, soil texture, mantle thickness, homogeneity, and structural control. Thus, from an evaluation of these patterns, one can deduce compositional identities such as igneous, metamorphic, sedimentary (sandstone, limestone, shale, massive beds, thin beds, interbedded), soil types, and properties such as hard, soft, dusty, quick, sticky, unstable, etc. A fundamental principle is that like patterns, wherever they occur, indicate like materials and/or conditions, and unlike patterns indicate unlike materials and/or conditions. The basics of this manual analysis procedure are described in various publications (e.g., Belcher, 1943; Frost et al., 1953; Rinker and Corl, 1984). For obtaining this type of terrain information, the manual analysis of stereo imagery is still state-of-the-art. Digital analysis of spectral data contributes little direct information. Digital techniques such as band combinations, enhancement, etc., can, however, improve pattern boundaries for visual observation.

1.2 TARGETING

Targeting refers to the detection and, hopefully, the identification of specific features, items, or conditions. For success, the target must have some characteristic that differs from its background and which cannot be confused with any other feature in the field of view. For point targets, this is seldom the case. The prediction of detectability is based on physics, and more often than not, this can be done successfully. But, more often than not, identification is iffy, mostly because of signals that, in the spectral band of use, look like the target. For passive systems such as thermal infrared and thermal microwave, these issues are more complex than for active systems. In general, the more cluttered the image scene, the more difficult it is to identify point source targets. Detection based on shape, size, and arrangement includes examples such as roads, airports, dams, vehicles, crop/field patterns, structures, and urban areas; and such are usually easier to identify by manual analysis. In addition to shape, differences can also be based on color, spectral reflectance, spectral emittance (temperature), luminescence, acoustical reflectance and emittance, magnetic fields, etc. Application examples include road type (asphalt or cement concrete), diseased vegetation, stressed vegetation, flood boundaries, wetland areas, thermal springs, thermal plumes from power plants, oil slicks, hot spots in burned areas, alteration zones, number of lakes in a region, camouflaged sites, and military units and equipment. Included in targeting are the applications of change detection and monitoring, e.g., seasonal changes in wetlands, desertification, flood and fire damage, alteration of land use, forest clearing, extent of pack ice, etc. Although aerial photography and multiband images are used in these tasks, it is here that digital spectral imagery and computer techniques of digital analysis become important. Spectral data define the

molecular characteristics of the surfaces, whereas shape, especially stereoscopic shape, identifies object types. For example, the spectral reflectance characteristics of a sand sheet, barchan dunes, a dome dune field, and a sand-veneered playa are similar—similar to the extent that they would be grouped as an entity. Shape reveals that: two are plains, one of them to be avoided (the playa); the isolated hills are barchan dunes that can provide sites for cover and concealment, observation, etc., and with excellent support for vehicles on the interdunal surface; and, the dune field will support cross-country movement by HMV type vehicles, but not heavy trucks.

For targeting and change detection applications, military or civil, the more bands available to examine the scene, the better the chances for detection and identification. A camouflaged target can resemble the terrain visually, photographically, and thermally, but be a mismatch in the radar bands; or, match in the radio frequencies, but not in the thermal infrared; or match in radar and thermal infrared, but show a mismatch in its reflected solar spectral signature.

2. RADIATION - THE CARRIER OF INFORMATION

2.1 BASIC CHARACTERISTICS

Until 1819, electricity and magnetism were thought to be unrelated independent forces. In that year, the results of experiments by Hans Christian Oersted, a Danish physicist, proved that these two forces were not independent—but were intimately bound together. These two fields will always be present together, at mutual right angles, coalesced into an entity known as the electromagnetic field, with the electric field associated with voltage, and the magnetic field associated with current. In the 1860s, James Clerk Maxwell developed his famous set of four equations that established the relations between electricity and magnetism under all conditions; combined electricity, magnetism, and light into a single concept; and showed the existence of self-propagating electromagnetic waves. The propagation results because a time-varying electric field induces a time-varying magnetic field which, in turn, induces a time-varying electric field—and on to infinity, or until the energy content becomes vanishingly small. This continuous generation which takes place at the leading edge can occur only so fast, no more and no less, a defining rate at which each field can produce the other. It is this that establishes the speed of travel, and why it is a constant in a given medium. One result of Maxwell's equations, which astounded physicists at the time, was that the speed of propagation predicted by the equations for an electromagnetic field was the same value as the speed of light, which had already been measured. The speed of a wave motion is equal to the wavelength multiplied by the frequency. Equation 1 states it for electromagnetic waves. Figure 3 is a sketch of a changing electric field to illustrate concepts and terminology. For simplicity, the magnetic field, which would be in phase with the sketched waveform, but perpendicular to it, is not included.

Anything that influences either the electric component or the magnetic component alters the characteristics and response of the electromagnetic field. In passing through matter, the attribute that interacts with the magnetic field is called the relative permeability (symbol μ), and that which interacts with the electric field is called the relative permittivity (symbol ϵ). As shown in the Fig. 3 equation, this combined field travels through space at a constant speed for all frequencies. In condensed matter, however, the speed, or more properly the phase velocity, is slower for all frequencies, but not uniformly so, and is expressed by the following equation:

$$Velocity = \frac{c}{\sqrt{\mu\epsilon}} \qquad (1)$$

c = speed of light in vacuum.
μ = mu, relative permeability.
ϵ = epsilon, relative permittivity (dielectric constant).
The quantity $\sqrt{\mu\epsilon}$ is the index of refraction.

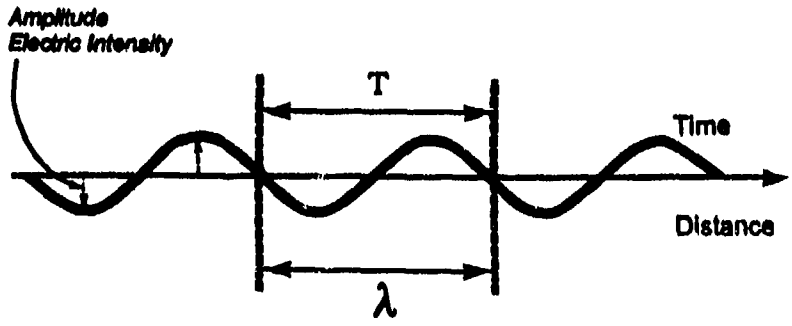

$$c = \lambda \nu$$

Figure 3. A representation of a time varying electric field. λ is wavelength. T is period (time per cycle), and c is speed of light, which in free space is about 3×10^{10} cm sec^{-1}, or about 186,000 miles per second. A useful relation for quick calculations is that light travels about 1 ft per nanosecond (10^{-9}sec).

The magnetic permeability of a vacuum is set at 1. Because most materials have a permeability close to one, the magnetic component of the electromagnetic field is usually ignored, and the index of refraction is considered to be the square root of the dielectric constant. Thus, the defining characteristic of electromagnetic radiation is the frequency of oscillation of the electrical field, which runs from the infinitesimally small to the infinitely large.

This spread of frequencies, known as the electromagnetic (EM) spectrum, is portrayed in Fig. 4. The division into subunits of radio, microwave, infrared, etc., is strictly arbitrary, because there is no fundamental difference between them. The division is based, in part, on the different experimental techniques used, and in part on the fact that, historically, they were studied separately, and were once thought to be distinct entities. Spectral bands can be specified by numbers for frequency (cycles per second) and wavelength (Angstroms, nanometers, microns, feet, miles, etc.), or by words. Words that designate frequency locations are radio terms such as Low Frequency (LF), High Frequency (HF), Very High Frequency (VHF), Ultra High Frequency (UHF), and Extraordinary High Frequency (EHF), at which point they ran out of superlatives. On the wavelength side, amateur radio operators use the terms 1 m band, 10 m band, etc. General descriptors for various portions of the EM spectrum, going from high frequency to low, or from short wavelengths to long, include: gamma ray, x-ray, ultraviolet, visible, infrared, microwave, and radio. The visible part of the EM spectrum covers the approximate wavelength range of 400-700 nm. It is not a sharp cutoff at the long wavelength end, and many people can perceive photons with wavelengths well beyond 700 nm. The 400-500 nm band is called blue, the 500-600 nm band green, and the 600-700 nm band red. Wavelengths shorter than 400 nm fall in the ultraviolet region, and wavelengths longer than 700 nm are in the infrared domain, which extends out to a wavelength of 1 mm. Beyond this is the microwave region, which contains the radar bands. Over this extreme, from low frequency radio waves to high frequency γ-rays, there is an enormous difference in photon energy via the relation $E = h\nu$. We are immersed in an ocean of radio waves, but of such low energy that the effect on body tissue is little, or none – although subject to debate. At the high frequency end, γ-rays have such high energies that they are dangerous. Also shown at the top of Fig. 4 are the general locations of absorption due to electronic, rotational, and vibrational processes.

The sun, the most used energy source in remote sensing, is a blackbody radiator, operating at an average surface temperature of about 5800° K, and emitting energy from the short wavelengths of x-rays, through the ultraviolet, the visible, the infrared, and out to the longest wavelengths in the radio region. On an intensity *versus* wavelength plot, the curve peaks at about 480 nm, i.e., more energy is emitted at this wavelength than at any other. Some 96 percent of the sun's energy, however, is emitted at wavelengths shorter than 2.5 μm. At wavelengths longer than this, one enters the thermal infrared domain and the need for different types of detectors. Although there is still a solar component, the amount is small compared to the

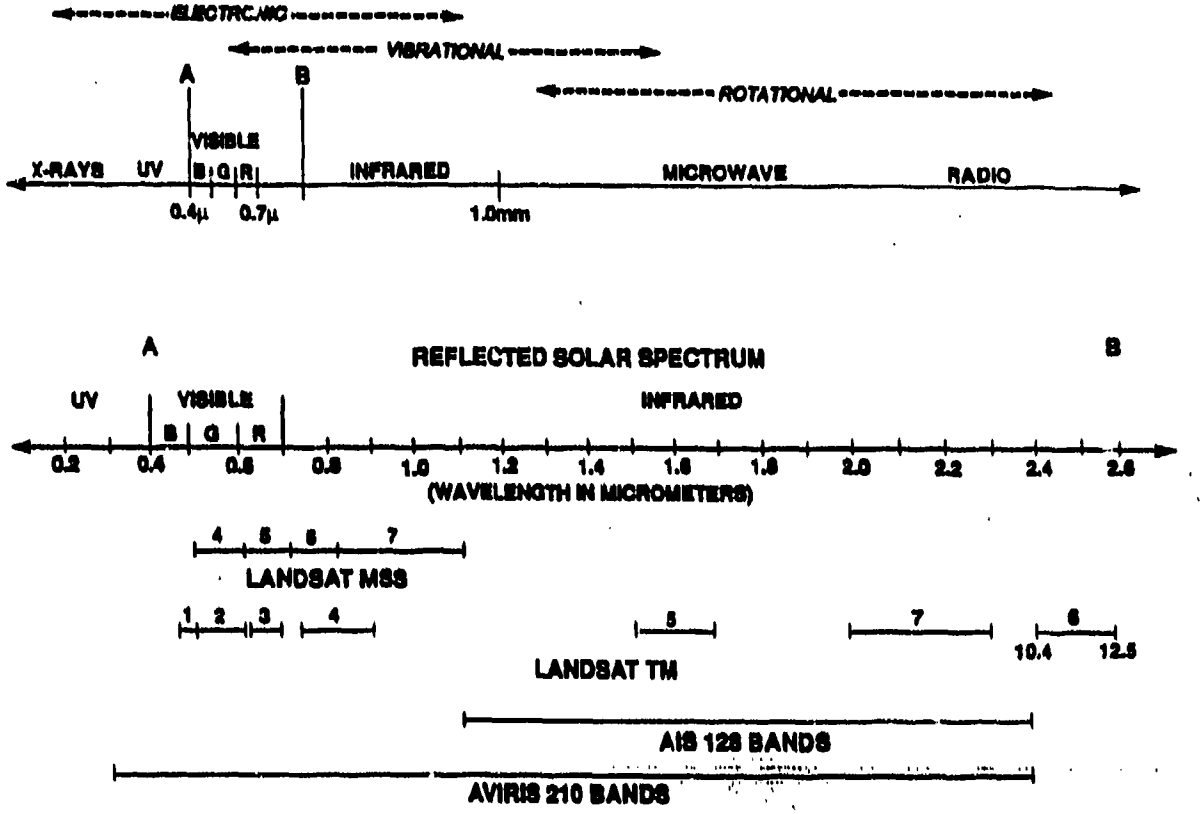

Figure 4. Electromagnetic spectrum. The top diagram locates various bands in a relative sense. Above it are general locations for electronic, rotational, and vibrational absorption processes. The next line down is an expansion of the AB portion. Below are approximate band locations for some of the operational multispectral and hyperspectral systems.

thermally emitted signal. For wavelengths shorter than about 350 nm, the atmosphere greatly attenuates the incoming photon flux. Thus, the reflected solar spectrum is generally considered to cover the 0.4 to 2.5 μm range; a spread that contains about 84 percent of the incoming solar energy, and which is probably the most used band in the electromagnetic spectrum.

2.1.1 Bandwidth and Pulse Duration

When electromagnetic energy is transmitted as a continuous series of pulses, the spread of frequencies required to emit the pulse is determined by time duration of the pulse. Pulse Duration (PD) times the Bandwidth (BW) is approximately equal to 1. A basic law of physics.

$$PD \cdot BW = 1 \tag{2}$$

Pulse Duration is the reciprocal of the Bandwidth, and *vice versa*. The narrower the band of frequencies, the longer the pulse duration. The shorter the pulse in time, the greater the spread of frequencies needed to get the energy out. As the time duration of the pulse becomes shorter, the pulse must shift to ever higher frequencies.

$$BW = \frac{1}{PD} \tag{3}$$

$$PD = \frac{1}{BW} \tag{4}$$

Wave packets can be created by adding together waves of different frequencies that have no beginning and no end. Taking a central frequency, and adding to it frequencies that are a little lower, and frequencies that are a little higher, the waves interfere with each other, constructively and destructively, to create a series of pulses, or wave packets, that travel through space. Between these packets, the electric and magnetic fields of the wave add vectorially to reduce the field to zero (destructive interference). The more frequencies added, the shorter the time duration of the pulse, and the less space it will occupy. Interference is a property of waves, whether they are visible light, radio frequencies radiating from an antenna, acoustical waves from a loud speaker, or pressure waves in water; and, it is basic to explanations for bandwidth, focus, and resolution.

For a monocycle radar we developed for measuring thin ice thicknesses, the pulse had to be short enough to resolve the two reflections, one from the top (air/ice), and one from the bottom (ice/water) surfaces of an ice layer of 10-15 cm. At the speed of the signal in ice, this required a pulse of 2.5 nanoseconds duration, with a corresponding bandwidth of 500 megacycles. In 1962, that was considered a very short pulse. Since then, techniques and hardware have progressed to the point that ultrashort pulses can now be generated in the femtosecond domain (10^{-15} sec). Fork (1990) reports on pulse durations of 6 femtoseconds. To put this in perspective, a 1 sec pulse occupies 186,000 miles of space—a nanosecond pulse occupies 1 ft of space—and a 6 femtosecond pulse occupies about 1.8 μm of space—about twice the length of a bacterium such as *E. Coli*. Light forming such a brief pulse must contain the full complement of the visible spectrum (blue, green, red), plus ultraviolet and infrared frequencies.

2.1.2 Interference

In order to collect photons and record an image, some kind of an optical element is needed to bring them into the system, such as a lens, or an antenna. This introduces the factors of focus, resolution, beamwidth, and side lobes, all of which depend on constructive and destructive interference phenomena associated with waves. Figure 5A illustrates wave interference, or diffraction. A wave front passes through the two slits, S_1 and S_2, and arrives at Point P. In the lower example, P_1 is exactly 10 wavelengths from S_1, and from S_2. The troughs and crests, produced simultaneously at the sources, arrive at P_1 at the same time so that they add together (constructive interference) to create a strong field, or wave, at P_1, stronger, or brighter, than either of its components. These waves are said to be in phase. In the upper example, S_2 to P_2 is 10 wavelengths, and S_1 to P_2 is 10½ wavelengths. When the waves arrive at P_2, they are 180°, or ½ cycle out of phase. A crest from S_2 arrives with a trough from S_1. The fields cancel each other (destructive interference), and there is no field at P_2—it is dark. If the difference between the two paths is one wavelength, or two, or three, they arrive in phase again, and form a brighter area, as in the lower illustration. A view of the image plane in Figure 5B would show a central bright spot surrounded by alternate dark and light zones, the light zones rapidly diminishing in brightness. The change from bright to dark to bright is a gradient, not a step, because the ratio between crest and trough varies constantly as one progresses along the image plane between the bright and dark extremes. Obviously, the waves cannot be brought to a focus at a precise point—they will spread out over an area. This interference pattern directly determines focus, resolution, instantaneous field of view (IFOV), or beamwidth, as in radar.

2.1.3 Focus

The term is widely understood in an intuitive sense. But, what is meant in an exact sense? In Fig. 6, a sequence of plane waves of light coming from point S in the object plane travels to the lens, passes through all parts of it, and proceeds on to point I in the image plane. In order for point S to be in focus in the image plane, the lens must be ground so that the number of wave cycles is exactly the same for every path through the lens to point I. The first point of contact of the lens with a wave front is the bulge of the lens on the axis. At that point, the wave enters the glass, slows in accordance with the index of refraction, and passes through the thickest part of the lens to emerge on the other side where it resumes its former speed and eventually arrives at I. Another part of the same wave front passes through the outer edge of the lens *en route* to I, and this path is longer than the one through the center of the lens. But, the longer time in the high speed air path, coupled to the shorter time in the slower speed glass path, adds up so that it arrives at I at exactly

the same time as that which went through the center of the lens. To be in focus, the number of waves between object and image points must be exactly the same through all parts of the lens. An excellent discussion on the nature of electrons and waves can be found in Pierce (1956).

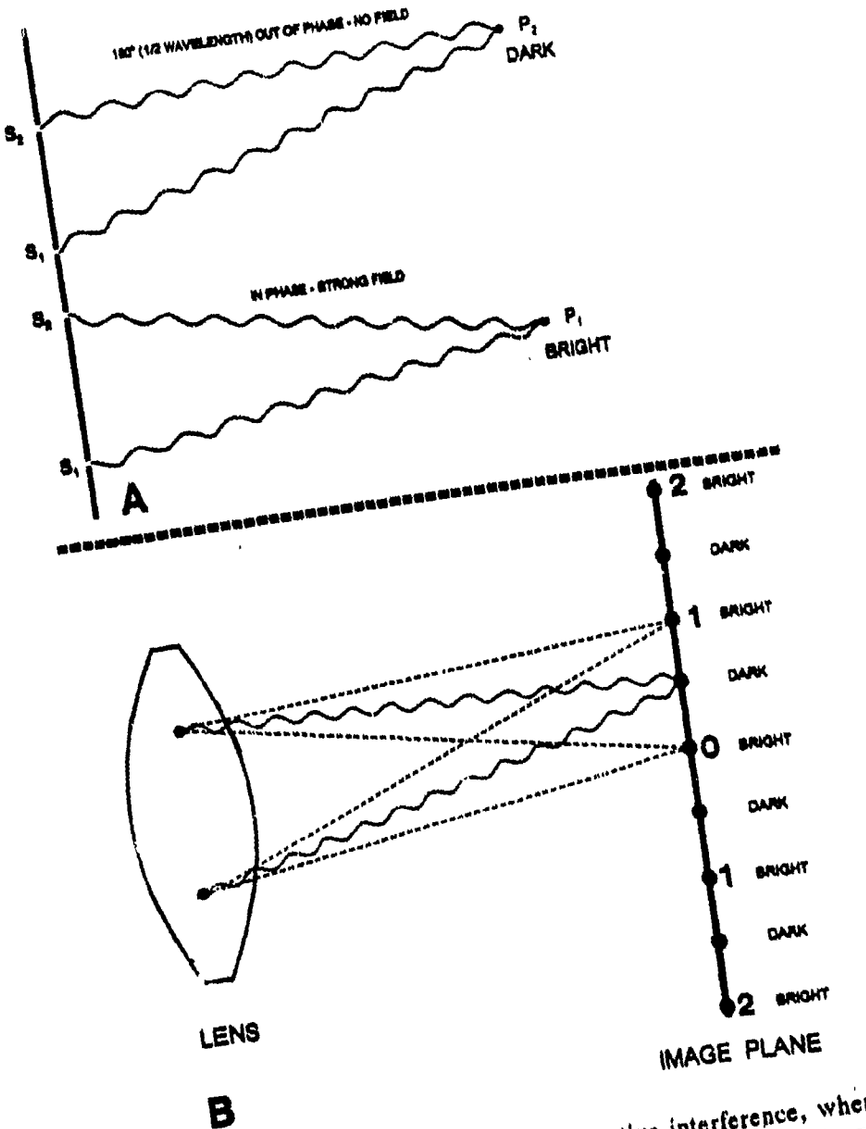

Figure 5. Interference. The lower part of A illustrates constructive interference, where each path has the same number of waves, 10 in this case, and combine at P_1 to produce a strong field. They are in phase. The upper drawing of A represents destructive interference. Path S_2-P_2 is 10 waves, and path S_1-P_2 is 10½ waves, i.e., the waves are ½ cycle out of phase. The crest of one meets the trough of the other, canceling the electric field at that point. In B, light from the lens, impinging on the image plane, forms a central bright zone surrounded by alternate dark and light zones. At 0, the waves arrive in phase and create a strong field. Going up or down, the path lengths begin to differ. Where they differ by one half a cycle, the fields cancel, and darkness results. Continuing up or down, the paths will eventually differ by 1 wavelength, and will add constructively to form a brighter zone. Intensity is maximum at 0, and decreases at each succeeding bright zone. The size of the central spot determines the resolution.

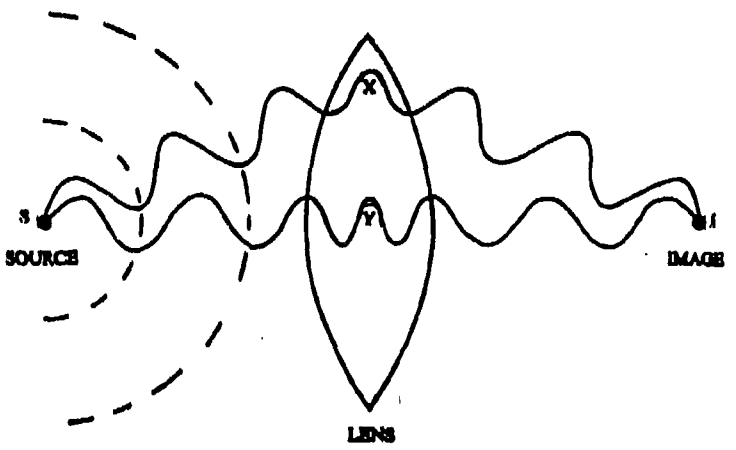

Figure 6. Focus. In focus means the same number of wavelengths in each path through the lens to the image point. The lens must be ground to make this so. At the edge of the lens, the longer path in high speed air, coupled to a shorter slow speed path in the lens, exactly matches, in time, the shorter on-axis path length where the wave spends more time in glass, and less time in air.

2.1.4 Resolution

The explanation for resolution also rests in the interference properties of waves, as illustrated in Fig. 7. Light coming from an object to the left of the lens is not shown. We pick it up at the lens and follow it to the image. At 0, the waves are in phase and form a bright spot. Proceeding up, or down, from 0, the

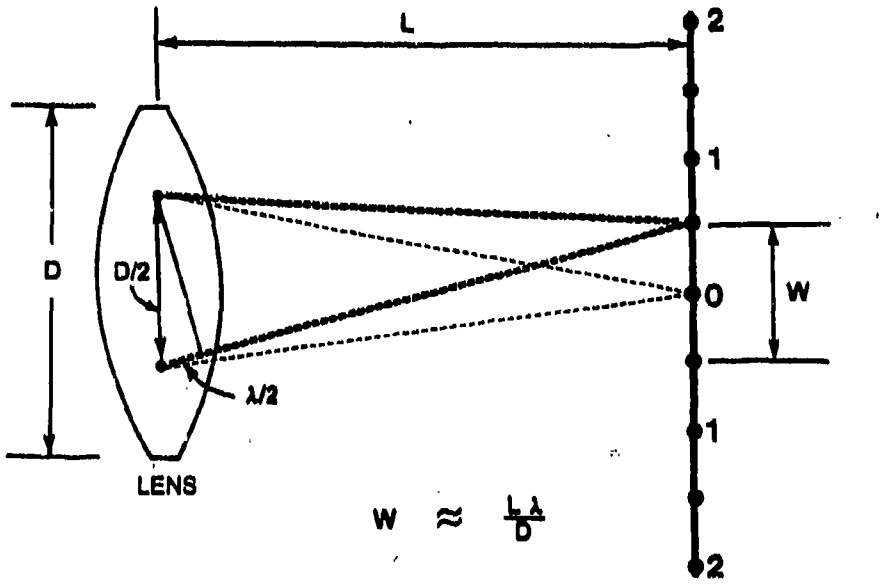

Figure 7. Resolution. The numbers to the right of the image plane refer to bright zones, with 0 being the main lobe, and 1 and 2 the side lobes. The dots between mark locations of zero fields, or dark zones. W represents a dimension of the main lobe, or bright spot, which can be considered as a resolution element, e.g., IFOV, beamwidth, etc. Because L is so much larger than W and λ, geometrical relations can be established as shown in the equations.

intensity of the light decreases until a zero field is encountered. At that place, the waves are one-half cycle out of phase, and the fields cancel each other—no light. Progressing further, up or down, the light becomes gradually brighter until it reaches another maximum at 1, where one path is one wavelength longer than the other. They are again in phase. Continuing up or down, the waves will slip into phase at 2 to produce another bright zone, and so on. If one could look at the image plane face on, there would be an intense bright spot at 0, surrounded by an alternating series of dark and bright circles. The spot at 0 is the brightest, i.e., it has the maximum amplitude. The first bright zone, or ring, surrounding 0 has an intensity of about one fifth of the max. The second bright zone is about one eighth of max. If we replace the lens with an antenna, as in radio or radar, these zones are called lobes. The one at 0 being the main lobe, the next being the first side lobe, the next the second side lobe, and so on. In his book, Kock (1965) provides excellent discussion and sketches associated with the fundamentals of wave motion, as well as photographs of the diffraction structure of acoustical waves and microwaves. The photographs show what the equations predict.

The central bright spot is the smallest point dimension that can be produced by the element, and represents the resolution of the lens, or antenna, except in the latter case it is called beam width. If two points are so close together that their central bright spots merge, they cannot be resolved. Also note that there is not a sharp division between field and no field, i.e., between bright and dark. Thus, if focused for maximum resolution, the image will have a somewhat fuzzy look. There are ways to estimate approximate limits for this central bright spot. Figure 7 (based on Pierce, 1956) shows a lens of diameter D focused on point 0, which is some distance L from the lens. Arbitrary points in the lens are a distance of D/2 apart. Point 0 represents the center of the bright spot, or main lobe, where the waves are in phase. Points 1 and 2 above and below 0 mark locations of the other lobes, or zones of brightness. The points between the numbers represent dark zones. The distance W represents the central area in which the in-phase waves arrive, or leave. Because L is so vastly greater than either W or λ, then very nearly:

$$\frac{W}{L} \approx \frac{\frac{\lambda}{2}}{\frac{D}{2}} \approx \frac{\lambda}{D} \tag{5}$$

$$W \approx \frac{L\lambda}{D} \tag{6}$$

W defines the resolution element formed by light coming from the lens D. It also defines the resolution element over which a collecting lens, or antenna, can receive photons of a given wavelength. It says that for a lens of diameter D, collecting photons of wavelength λ from a surface L distance away, the smallest recordable area (resolution cell) has a diameter of W. It also says that for an antenna of length D, emitting microwaves of wavelength λ, the width of the beam at distance L from the antenna is W. If L coincides with the surface being illuminated, then W is one dimension of the IFOV for that system. Also, the equation says that for a loudspeaker of diameter D emitting an acoustical signal (pressure wave) of wavelength λ (or frequency ν), the width of the beam L distance away is W. Holding D and L constant, but changing the tone to $\lambda/2$, i.e., doubling the frequency, which is an octave, W is one half its former value. Thus, the beam width is different for different tones coming from the same speaker. As a beamwidth example, take a radar with a 3 m long antenna operating at 10 cm wavelength. The width of the beam 10 km away will be about 330 m. A Synthetic Aperture Radar (SAR) allows one to synthesize what the radar interprets as a very long antenna—with resultant narrow beamwidths. Note the relation of the shape of the resolution element to the shape of the emitter, or collector. The narrowest part of the beam will be parallel with the longest dimension of element, and the widest part will be perpendicular to this. Table 1 lists some resolution elements for different systems. Beamwidth can also be derived in degrees if λ and D are expressed in the same units.

$$W(degrees) \approx \frac{51\lambda}{D} \tag{7}$$

TABLE 1. SOME RESOLUTION AND BEAMWIDTH EXAMPLES

Refer to Equation 6. Lambda (λ) refers to wavelength, ν to frequency, L to distance or range, D to diameter of lens or length of antenna, and W to resolution or beamwidth. The lower set is for acoustical waves. Values are approximate.

	λ	L	D	W
MICROSCOPE	0.55 μm	1 mm	2 mm	0.3 μm
BINOCULARS	0.55 μm	1 km	40 mm	14 mm
TELESCOPE	0.55 μm	3.5 X 10^7 mi.	1 ft	63 mi.
RADAR	10 cm	2.5 km	3 m	83 mi.
RADAR	3 cm	2.5 km	3 m	25 mi.
	ν			
LOUDSPEAKER	20 kHz	10 ft	1 ft	0.5 ft
LOUDSPEAKER	11 kHz	10 ft	1 ft	5.1 ft
LOUDSPEAKER	11 kHz	10 ft	3 in.	20.4 ft
LOUDSPEAKER	1 kHz	10 ft	1 ft	56 ft

2.2 ABSORPTANCE AND REFLECTANCE

When electromagnetic energy falls on a material (gas, liquid, or solid) several things can happen. What happens depends on the electrical properties of the materials, i.e., the index of refraction, or dielectric constant. In turn, this is a function of the oscillation frequency of the incoming electric field. If, in going from one medium to another, the radiation encounters a change in electrical properties that takes place in a distance less than its characteristic wavelength, then something must happen to that radiation—it cannot continue as it was. It will undergo, singly or in combination, transmission, reflection (scattering), refraction, or absorption.

Incident radiation is absorbed if the photon energy matches an energy separation between two stationary states of the molecular components. Absorption characteristics, such as center frequency location, band depth, etc., carry the information needed to identify materials, and establish conditions, such as vegetal stress. In the laboratory, one can measure absorptance, as well as transmittance, reflectance, and emittance. With airborne and space systems, one can collect only those photons that have been reflected, and infer what has been absorbed by evaluating what is missing from the beam reflected to the sensor.

All frequencies can undergo conversion to thermal energy, a process of broad-band absorption, as in solar heating of the earth, solar cookers, and microwave ovens. Narrow band absorption is responsible for the colors seen from surfaces, or through filters. A yellow filter looks yellow because it absorbs the blue part of the visible spectrum, and passes the green and red bands—a combination that causes the sensation in our eye called yellow. Because a yellow filter does not transmit blue photons, it is also called a minus-blue filter. In order to absorb energy, the structural components, i.e., electrons, atoms, or molecules, must be capable of displacement motions that can occur in the time domain of the frequency of the radiation. Absorption of photons raises that component to a higher energy level, whereupon it will either return to its former lower energy state by emitting radiation, or transfer energy to other mechanisms. Absorption processes are classified as electronic, vibrational, rotational, and oscillatory; and the energy domains of these processes overlap. Electrons, being the lightest and fastest of the components, capable of resonating at very high frequencies, are involved in the absorption and emission of high frequency radiation, from gamma-rays to the near infrared. Molecular and atomic components, being massive, have slower displacement movements, and resonate only at lower frequencies. Vibrational absorption modes start in the visible and extend out into the millimeter wavelength domain. Rotational absorption begins in the middle infrared and extends out to radio waves. These regions are shown in Fig. 4.

When matter is condensed into a solid state, the electron orbitals are shoved together, become smeared, and lose the fine-structure details associated with electronic spectra. There is also loss of ability for rotational displacements. Vibrational processes become dominant, and the spectral bands of the fundamental modes occur in the middle and far infrared. For the most part, the only bands that can appear in the near infrared are those associated with overtones, or combinations of the fundamentals. Thus, the reflected solar region of the spectrum, the basis for hyperspectral sensing, carries little to no information about fundamental modes.

A normal, or fundamental, mode of vibration is one in which the component nuclei of the molecules undergo simple harmonic motion at the same frequency, in phase, but with different amplitudes. If one knows the molecular structure, there are quantum mechanical computations involving masses and force constants that can be used to determine the vibrational frequencies, and thus the frequencies of absorption. Conversely, one can measure the absorption spectra, and determine what must be the molecular structure. Details of such calculations are in various texts on spectroscopy, e.g., Hollas (1982). Background material, particularly with reference to minerals, can also be found in a series of excellent papers by Hunt and Salisbury (1970).

To show some of the relations between absorption and structure, consider the water molecule in Fig. 8. It is a bent molecule with C_2 symmetry, and has three normal modes of vibration, all in the infrared: ν_1, symmetrical OH stretch; ν_2, the H-O-H bend; and ν_3, asymmetrical OH stretch. These are the fundamentals, and they take on different vibrational values for the vapor, liquid, and solid states. For the vapor state, these values, taken from Hollas (1982) and expressed as wave numbers are: ν_1 = 3657.1 cm^{-1}, ν_2 = 1594.8 cm^{-1}, and ν_3 = 3755.8 cm^{-1}. Equivalent wavelengths for these wave numbers, expressed in microns, are: 2.734, 6.270, and 2.662. Although single values of wave numbers are used in this discussion, the vibrations of a fundamental mode are spread over a range of values. Table 2 lists absorption bands for the vapor, liquid, and solid phases. Fundamental values for the liquid and solid states are from Hunt and Salisbury (1970). The lower part of the table lists absorption bands associated with overtones. The $2\nu_3$ band and the $\nu_2 + \nu_3$ band are characteristic absorption bands of water, and usually referred to as the 1.4 μm and 1.9 μm bands. When 1.4 and 1.9 are both present, it indicates undissociated water, i.e., plain water, such as water of hydration, water trapped in crystal lattices, or cellular water in tissue. The 1.4 band by itself indicates OH groups other than those associated with water, such as the hydroxyl group in alcohol.

The recording of the reflected component of radiation is the most common form of remote sensing, and the sun is the most frequently used source of illumination. The reflected solar spectrum (0.4-2.5 μm) supports sensors such as cameras, the Landsat Multispectral Scanner (MSS) and Thematic Mapper (TM) bands 1, 2, 3, 4, 5, and 7 (band 6 being a thermal infrared band), SPOT, and the hyperspectral systems, such as the Airborne Visible Infrared Imaging Spectrometer (AVIRIS). The tone differences that define boundaries of shapes, soil changes, and the highlight and shadow tones are due to different amounts of radiation reflected to the sensor from the various surfaces.

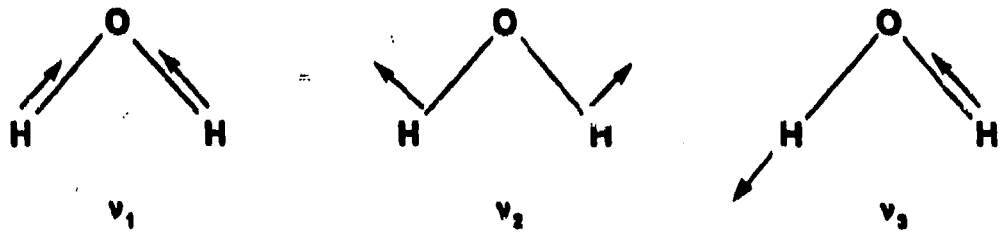

Figure 8. The three fundamental modes of vibration of a water molecule. The arrows indicate direction of the displacement. ν_1 refers to the symmetrical OH stretch, ν_2 refers to the H-O-H bend, and ν_3 refers to the asymmetrical OH stretch.

TABLE 2. ABSORPTION MODES

Wavelengths (in microns) associated with the fundamental and overtone vibration and absorption modes of the water molecule. The fundamental values for liquid and solid are from Hunt and Salisbury (1970), and for the vapor phase are from Hollas (1982). These are approximate values, because there is a spread of frequencies in the vibratory bands. Absorption spectra of the vapor phase will show numerous sharp bands caused by rotational fine structure. The loss of fine structure in the liquid and solid states is due to loss of rotational displacements.

Mode	Vapor	Liquid	Solid
Fundamentals (μm)			
ν_1	2.734	3.106	3.105
ν_2	6.270	6.079	6.06
ν_3	2.662	2.903	2.941
Overtones (μm)			
$2\nu_1+\nu_3$	0.903	0.902	1.016
$\nu_1+\nu_2+\nu_3$	1.110	1.135	1.212
$\nu_1+\nu_3$	1.349	1.379	1.510
$2\nu_3$	1.331	1.451	1.470
$2\nu_2+\nu_3$	1.439	1.454	1.501
$\nu_2+\nu_3$	1.869	1.965	1.988

The amount of radiation reflected from a surface depends on the wavelength of the light, its angle of incidence with the surface, the orientation of the sensor in relation to the surface and the illuminant, the material's molecular composition, and the surface structure. Molecular composition, however, sets the stage. A surface that reflects uniformly across the visible and photographic parts of the EM spectrum is called a neutral surface—i.e., it does not treat any one wavelength different from any other. For normal angles of illumination, no neutral material is a perfect reflector, i.e., 100 percent reflectance throughout the spectrum. Nor is it a perfect absorber, i.e., 0 percent reflectance. If it has a high reflectance, it is called white. If it has a low reflectance, it is called black. In between it is called gray.

Most materials reflect more at some wavelengths than at other wavelengths, e.g., a blue surface reflects blue light, and absorbs green and red, a yellow surface absorbs blue, and reflects green and red, and a green surface reflects green light, but absorbs blue and red. If three surfaces, e.g., blue, green, and red, reflect the same amount of photon energy, then a black and white photograph would show them with similar gray tones. Depending on the wavelength sensitivity of the film, they could be indistinguishable. A normal color film, however, is a multiband system. It has three bands, or channels, that separately document the intensities in the blue, green, and red bands, and displays the results as a color composite—showing that there are three different objects in the scene.

Figure 9 is a typical spectral reflectance response of healthy vegetation. In the visible part of the spectrum, the vegetation absorbs blue light, reflects some of the photons in the green band, and absorbs photons in the red band—thus, we see healthy leafy vegetal material as green, and it would be recorded as such in a normal color film. Healthy leafy vegetation is much more reflective in the infrared part of the spectrum, than in the visible; which is why, in black and white infrared photography, most vegetation shows as very bright tones. As indicated earlier, the dips at 1.4 and 1.9 μm are due to water absorption. As a plant loses water, these bands become shallower, and thereby provide an indicator of vegetation stress.

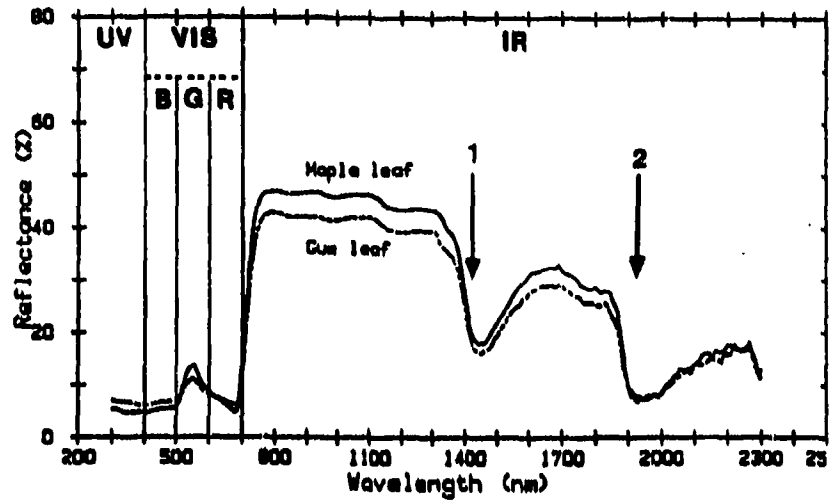

Figure 9. Reflectance characteristics of healthy vegetation. The reflectance in the visible part of the spectrum is mostly in the green band (500-600 nm), and is usually 10-15 percent. Reflectance increases rapidly in the infrared, reaching a maximum of around 35-50 percent. Arrows 1 and 2 indicate the water absorption bands at about 1400 nm and 1900 nm.

The infrared brightness of healthy vegetation has long been a useful characteristic for military targeting. In WW II, Eastman Kodak developed a film that could separate green painted camouflaged targets from surrounding green vegetation. Though a visual match, green paint is much less reflective in the infrared, than is vegetation. At that time, color films, such as Kodachrome and Ektachrome, were sensitive primarily to photons in the visible part of the spectrum. By extending the sensitivity of one of the three emulsion layers in Ektachrome film out to about 900 nm in the infrared region, Eastman Kodak developed the needed film, which was known as Camouflage Detection film, or CD film. With the proper filter, this film portrays green paint as green, and healthy vegetation as red. The emulsion with the extended sensitivity is the one sensitive to blue light, and which is coupled to the cyan dye. Increasing its sensitivity to infrared, out to 900 nm, also increased its sensitivity to the more energetic photons at double the frequency, or half the wavelength, i.e., 400-450 nm. The emulsion was about ten times more sensitive to blue light than to infrared. In order to tell which photons, blue or infrared, are responsible for the red tone, a yellow filter (Wratten 11, 12, or 13) is used to prevent blue light from entering the emulsion. With the blue light eliminated, the red response could be attributed to the vegetation—and any green painted object stuck out in stark contrast as green. Because the colors in an infrared photograph are not colors that eyes see in the scene, such a photograph is also called a false color image.

When vegetation is stressed, it loses much of its infrared reflectance. The stress can be induced by drought, flooding, chemical sprays, senescence, by biological infections such as the rust and wilt, or by infestations such as gypsy moths. The loss of infrared reflectance provides the basis for detecting the presence of stress, mapping its extent, and monitoring an area for change. Camouflage was, and still is, frequently made by cutting branches of trees and bushes to lay over the site—and this is effective, but only for a relatively short time. One response of the cut branch is that the leafy material loses its infrared reflectance faster than it loses its green reflectance. Even though looking equally green to the eye, the CD film shows the reflectance loss of the damaged vegetation as dark tones of red/green and green.

After WW II, CD film was evaluated for applications in geology, forestry, wetlands, land use mapping, and for detecting stressed vegetation. It became so useful that the consumer market constantly increased. Eastman Kodak improved the film, and changed its name to Ektachrome Infrared film (EIR). Adding infrared sensitivity makes a four channel system—blue, green, red, and infrared—analogous to Landsat TM bands 1, 2, 3, and 4. Taking the photograph through a yellow filter eliminates channel 1, the blue band, and the final

colors in the image result from mixes of intensities in the green, red, and infrared bands. With Landsat TM, the selection is made electronically. Of the seven bands available, one could select bands 1, 2, and 3, couple them to blue, green, and red guns and create a normal color image. One could also select bands 2, 3, and 4, couple them to the blue, green, and red guns, and create a false color composite image similar to the image from the EIR film with a yellow filter.

The quantity and quality of radiation falling on the terrain varies in relation to location, time of day, season, and atmospheric characteristics. On a clear day, the terrain is illuminated by two sources. One being a point source, the sun, and the other a diffuse hemispherical source, the sky. Skylight is blue, the result of atmospheric scattering of incoming short wavelength energy. Terrain exposed to sunlight is also exposed to skylight, receiving a double dose of blue. Terrain in shadow is illuminated with skylight only; thus, if one wants details within shadows, the blue component must be used. It is not exclusively blue light because sunlight of various colors can be reflected into a shaded area from vegetation, soils, rocks, buildings, etc.; but, blue is the major component. A yellow filter blocks blue light from contributing to the photograph, with the result that shadows are well defined with sharp edges and dark interiors—excellent for estimating canopy closure, or stem spacing and density, but poor for measuring canopy height where the ground must be seen. A black and white infrared film with a Wratten 87C filter that passes infrared radiation but excludes all visible light, gives the blackest shadows of all. Some filters pass two separate channels of radiation. A Wratten 47B (primary blue) passes blue light and infrared, absorbing green and the red. A Wratten 58 (primary green) passes green light and infrared, but rejects blue and red. Figure 10 shows the transmittance characteristics of these filters, and some results of different film/filter combinations. Coupled to the proper film, these filters provide a two channel system.

The set of aerial photographs in Fig. 10 compares an unfiltered Tri-X emulsion (XXX-0), which records all of the visual spectrum; infrared film with a Wratten 47B filter (IR-47B) which records both blue and infrared photons (a dual-channel system); and Infrared film with a Wratten 87C filter (87C), which excludes all the visible and records only the infrared (a single-channel system). These were taken some minutes apart. Although a few of the trees have started to drop leaves (early fall season), and some have changed color, much of the canopy shows as bright tones in the XXX-47B and IR-87C images because of the high infrared reflectance, as in location marked by Arrow 3. Cars in the shadow of the building .. easily visible in XXX-0 photograph, somewhat visible in the IR-47B, and not discernable in the IR-87C image (row 1). Arrow 2 points out one example of the bright sidewalks, visible in XXX-0 within the tree shadow, not discernable in the dual-channel XXX-47B, and reversed in tone in IR-87C.

In general, the reflectance of earth materials increases as one goes to longer wavelengths. In the ultraviolet and blue regions, most surfaces have a similar low reflectance. This is why photographs taken in ultraviolet, and in blue light tend to be flat—there is little contrast. Reflectance steadily increases going from blue, to green, to red, and to infrared. It is in the infrared region that brightness, contrast, and other interesting spectral features begin to develop. Figure 11 shows the reflectance characteristics of several playa surface materials, and indicates some of the more common absorption bands. The ordinates are percent reflectance. In the upper illustration, i.e., "A," the ordinate is not numbered because the individual reflectance records, which overlap, were offset vertically. In "A," the important indicative features are the locations of the various absorption bands along the wavelength axis. Strong water absorption bands at 1400 nm and 1900 nm are apparent for some of the materials. A record that shows both bands, i.e., 1400 nm and 1900 nm, indicates undissociated water such as water of hydration, or water trapped in the lattice. Molecular water, which is an important component in gypsum, has other absorption bands at 1000, 1200, and 1700 nm. These are overtones, i.e., combinations of the fundamental modes. These are marked as 1, 2, and 3. The lower illustration, "B," shows the effect of water on the reflectance properties of a silty loam playa soil. As the soil dries, the depth of the absorption bands becomes less, and the overall brightness increases.

A spectrometer measures light intensity on a wavelength basis. For reflectance measurements, this is usually done by measuring the amount of light of a given wavelength coming from the surface and comparing that value to the light itself, or to the light reflected from a reference surface of known reflectance

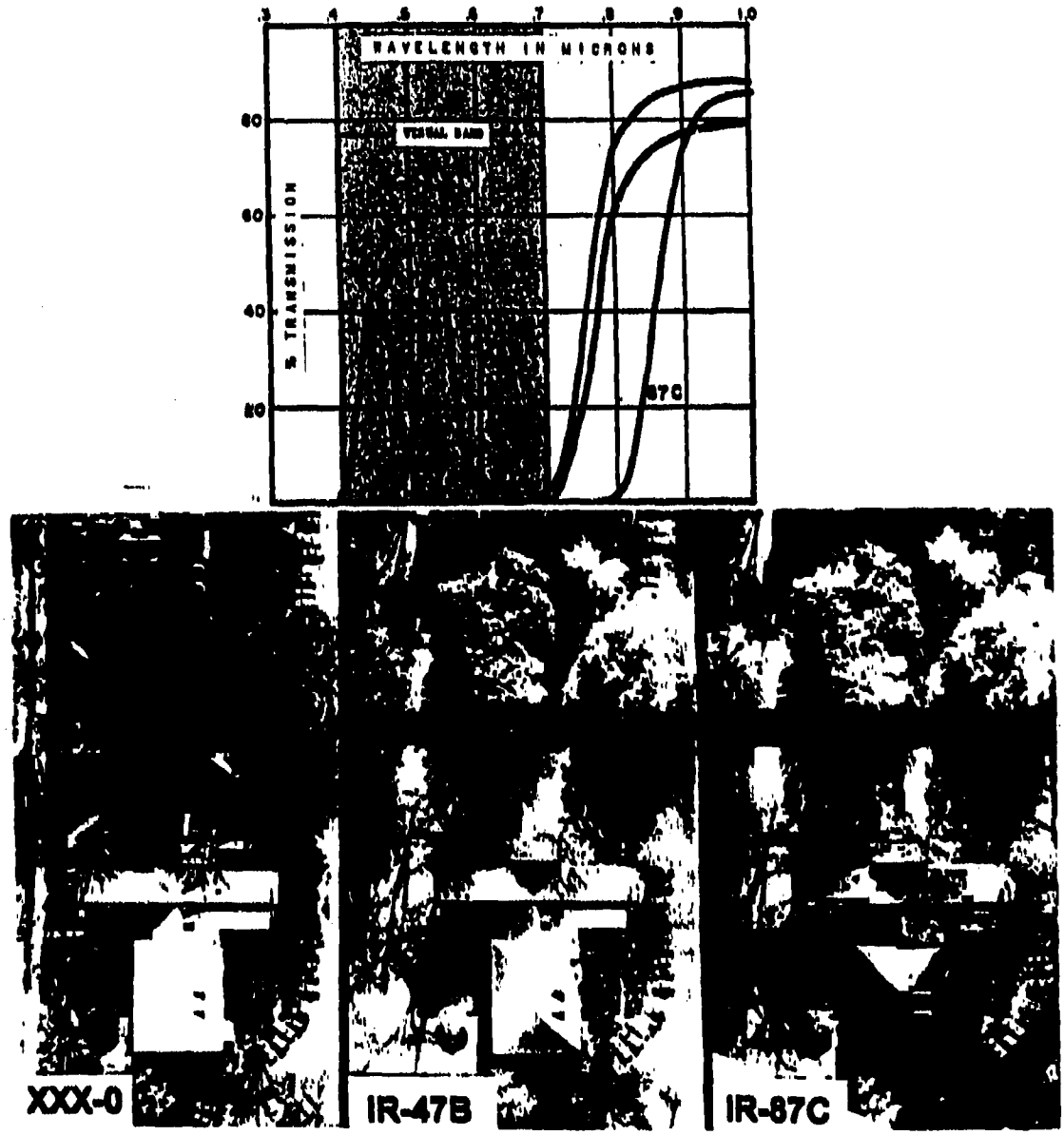

Figure 10. Top. Transmittance characteristics of Wratten filters 47B, 58, and 87C. The 87C passes only wavelengths greater than 800 nm. The 47B and 58 filters are two channel systems, passing the infrared band (> 700 nm), and about 45 percent of the blue band and 50 percent of the green band respectively. The bottom photos illustrate effects of these bands in recording shadow detail, or typing vegetation. Unfiltered Tri-X film (XXX-0) is a single broad band recorder, sensitive to blue, green, and red light. It depicts shadows as well as details within the shadows, which are illuminated with blue skylight. Arrow 1 points to automobiles within a shadow. They are visible, but less distinct in the IR-47B image, which records both the blue and infrared bands, and not visible in the IR-87C image which is the infrared band only. Arrow 2 marks sidewalk/grass contrast changes, and Arrow 3 marks area of high infrared reflectance in the trees. Infrared Aerographic film with an 87C filter (IR-87C) is a single broad band system, sensitive only to infrared photons—good for separating coniferous trees from deciduous ones, but useless for recording detail within shadows.

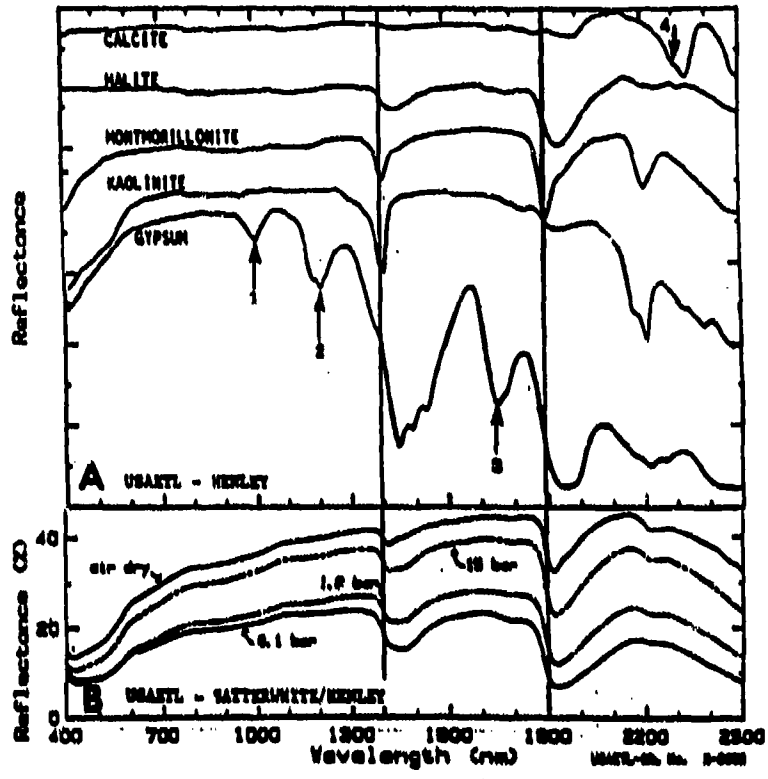

Figure 11. Playa surface reflectances. A. Reflectance measurements of playa surface minerals (Henley, 1988). The records are offset vertically to avoid overlap. The strong water absorption bands at 1400 and 1900 nm are apparent. When both are present, it indicates undissociated water (water of hydration, trapped water in the lattice). Kaolinite shows strong hydroxyl absorption at 1400 and 2200 nm but little at 1900 nm, which suggests a lack of bound water. Molecular water is important in gypsum, and its overtones and combinatorial tones account for the bands at 1000, 1200, and 1700 nm (Arrows 1, 2, 3). Calcite is fairly featureless except for the carbonate molecular vibration band at 2300 nm (Arrow 4), and sometimes a weak band at 2000 nm. B. Influence of moisture on a silty loam playa soil from Broadwell Lake, San Bernardino, April 1988 (Satterwhite and Henley, in edit).

characteristics. This comparison, or normalization, produces a plot of percent reflectance against wavelength. In the lab, physical setups can be varied to measure different kinds of reflectance, e.g., specular reflectance, bi-directional reflectance, total hemispherical reflectance, and diffuse minus specular. In the field, the sun is the usual light source, although halogen lamps are frequently used so that measurements can be made day or night, independent of sky conditions. Circumstances permitting, the procedure should be standardized. This includes a constant distance between spectrometer and the surface, and leveling the instrument and standard, and also target surface when possible. During the measurement cycle, stand away from the instrument to avoid adding a component of light reflected from clothing to the surface being measured. In addition to duplicate runs, take multiple measurements over the area or feature being measured. Do not assume homogeneity. To evaluate the spectrometer's performance in the field, keep a copy of the plot from the reference standard made right after the instrument was recalibrated. To check wavelength accuracy, one can use narrow band interference filters, clay minerals, etc.

A double field of view instrument collects measurements from both reference and target at the same time—one channel looking at the reference standard, and one channel looking at the target surface. Any variation in illumination during the measurement cycle is canceled because both surfaces are measured simultaneously. A single field of view instrument can collect only one set of measurements at a time. So,

measurements must be taken in sequence—first the standard, then the target. It takes a finite amount of time for an instrument to scan through the spectrum from 400 to 2500 nm, and if the illumination varies during the measurement cycles (reference and target), there will be an error in the results. If the spectral intensity distribution of the light falling on the target is not an exact match of that falling on the reference, then when the target data are normalized against the reference data, the resultant percent reflectance curve will not match that derived by a single field of view instrument. In the mid-latitudes, variation in solar intensity is significant in early morning and late afternoon. The least variation is in the noon zone, e.g., 1 to 1½ hours on either side of noon. In earlier field spectrometers, a measurement cycle could take over 10 minutes, which is ample time for variation to occur, particularly if one continues collecting measurements from other surfaces, and relying on the first reference reading for all. Measurement cycles were eventually shortened to seconds, and are now down to fractions of a second. Nevertheless, reference standards should be taken frequently.

2.2.1 Factors that influence reflectance

Although the molecular make-up of a material establishes the absorption characteristics, the recording of the reflected component is affected by: instrument calibration, variation in light characteristics (sun azimuth and altitude), atmospheric composition, surface structure, viewing angle in relation to the sun, surface attitude, etc. Instrument calibration is a separate issue. The intensity/wavelength distribution of sunlight at the earth surface varies with location, season, atmospheric composition, amount of atmosphere traversed, and time of day, changing most rapidly in morning and afternoon, and being more stable during midday, i.e., 1000 to 1400 hrs. Variation of irradiance with elevation is shown in Fig. 12A.

Surface structure and viewing angle are considered together because they are closely related in that the influence of surface structure is frequently dependent on viewing angle of the sensor in relation to the sun. Surface roughness can be defined in terms of wavelength of the radiation concerned. For a surface to be considered a high quality mirror, it must be flat to within about a quarter of a wavelength of the radiation to be used. Under this condition, most of the incoming radiation is reflected at an angle that equals the angle of incidence, i.e., specular reflection. If the surface variations exceed this, then proportionally more of the energy is scattered in other directions. This is called the diffuse component. As the surface variations increase, more energy is scattered in other directions, i.e., the diffuse component gets larger, and the specular component gets smaller. For remote sensors using reflected sunlight, the wavelengths fall between 400 nm and 2500 nm, or between 0.4 and 2.5 μm. Aside from still water, most surfaces have relief variations in excess of this, and are diffuse scatterers, e.g., leaves, bark, soil, rocks, concrete, paint, cloth, etc. Consequently, when viewing such surfaces from some point in space, the image tones can vary, even be reversed, as a function of viewing angle in relation to the sun. Looking at the ground in the up-sun direction, the sensor receives both a diffuse component and specular reflection component. Down-sun, the sensor receives diffuse minus specular, i.e., only the backscatter. If the surface variations have an orderly structure, the image patterns are influenced by sun azimuth as well. For example, the ridges and furrows of a freshly plowed field have relief on the order of 15 to 20 cm. Furthermore, it is an ordered relief, i.e., a pattern of parallel lines. If the sun's rays are parallel to the ridge pattern, the surfaces receive about the same amount of illumination and the image of the field would have an overall uniform tone. If the sun's rays are perpendicular to the ridge pattern, the field shows as a parallel series of highlights and shadows. X- and C-band radars would show a similar display. For L-band radar (25 cm wavelength), however, the plowed field would be a reflector, and would show as a dark area, an area of no return, from any angle of illumination.

Figure 12 shows the effect of changes in viewing angle of the sensor in relation to solar direction for a Halon standard (B), and for a coarse sand surface (C). For Fig. 12B, a leveled Halon standard was measured from two different viewing angles: with the spectrometer tilted 10° off vertical in the direction of the light source, which gave an increased component of specular reflection; and with the spectrometer tilted 10° off vertical away from the light source. A similar set of measurements for coarse sand particles (2-4 mm) is shown in Fig. 12C. These were normalized against the same reference, a vertical reading of the standard. The difference is not great, but it is 3-5 percent. These changes affect intensity only, not the location of absorption bands.

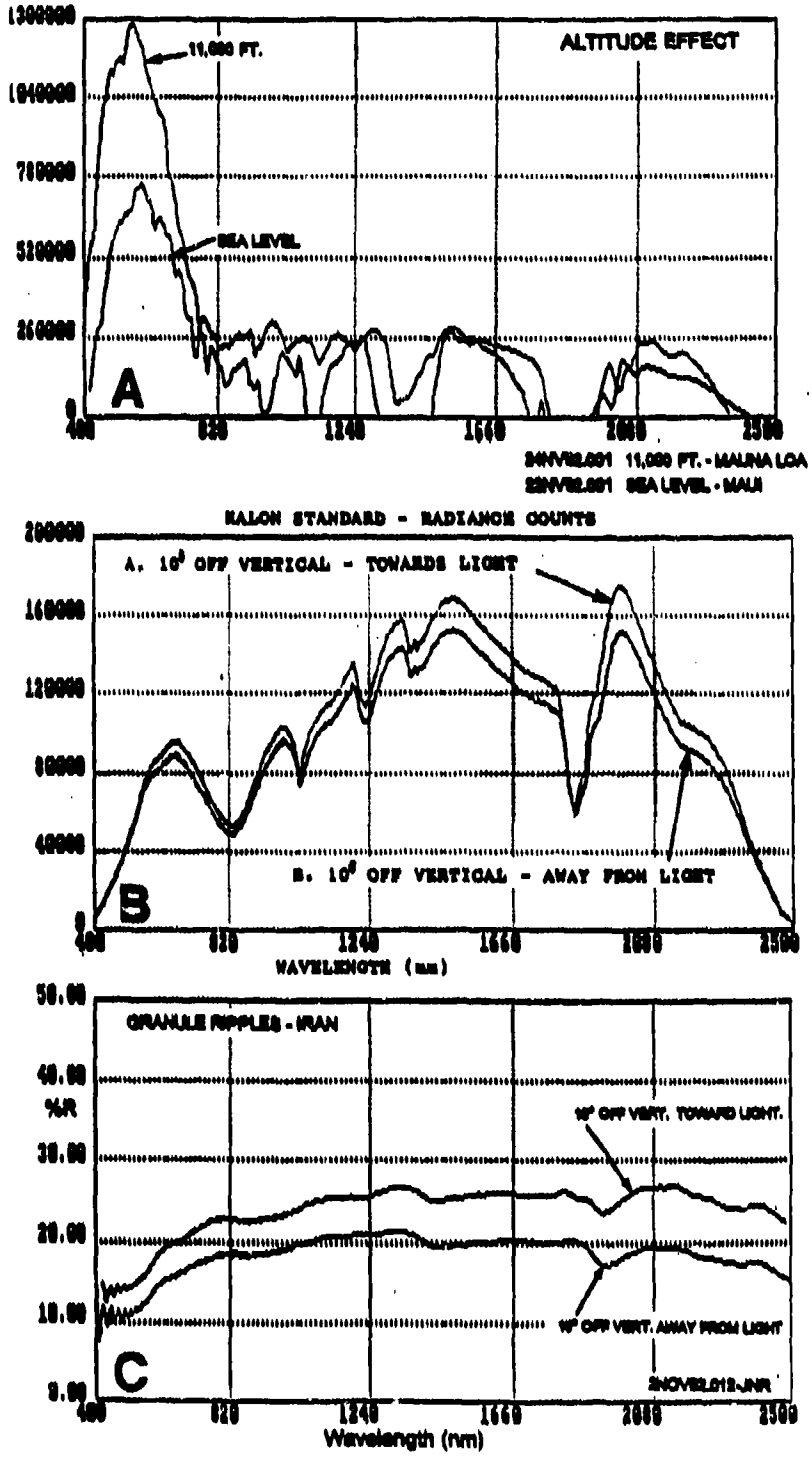

Figure 12. Variation of incoming solar radiation between sea level and 11,000 ft is shown in A. Variation caused by changes in viewing angle of the sensor in relation to the light source for a leveled Halon standard is shown in B. Results of a similar variation for a coarse sand surface (2-4 mm particle size) is shown in C. The two sand spectra were normalized against the same reference standard, a vertically measured Halon surface.

Figure 13 illustrates tone changes resulting from changes in viewing angle. The upper set of aerial photographs (A) is of an area on the south coast of Puerto Rico, showing water, beach sand, vegetation, shoals, etc. In exposure 164, this part of the frame has a viewing angle towards the sun, as indicated by the large bright area of sun glint, or "hotspot," on the water, which is the specular component of the sun's reflected radiation. Exposure 169 was taken several minutes later, while flying the adjacent parallel strip, and shows the same scene looking away from the sun. In 164, sun glint on the water masks shallow water bottom detail, which can be seen throughout the water area of image 169, especially in the sheltered bay, and shoal areas such as indicated by Arrow 1. On the other hand, sun glint makes the wave patterns conspicuous. On the point of land marked by Arrow 2, a small pond is depicted because of glint in image 164, but not visible in image

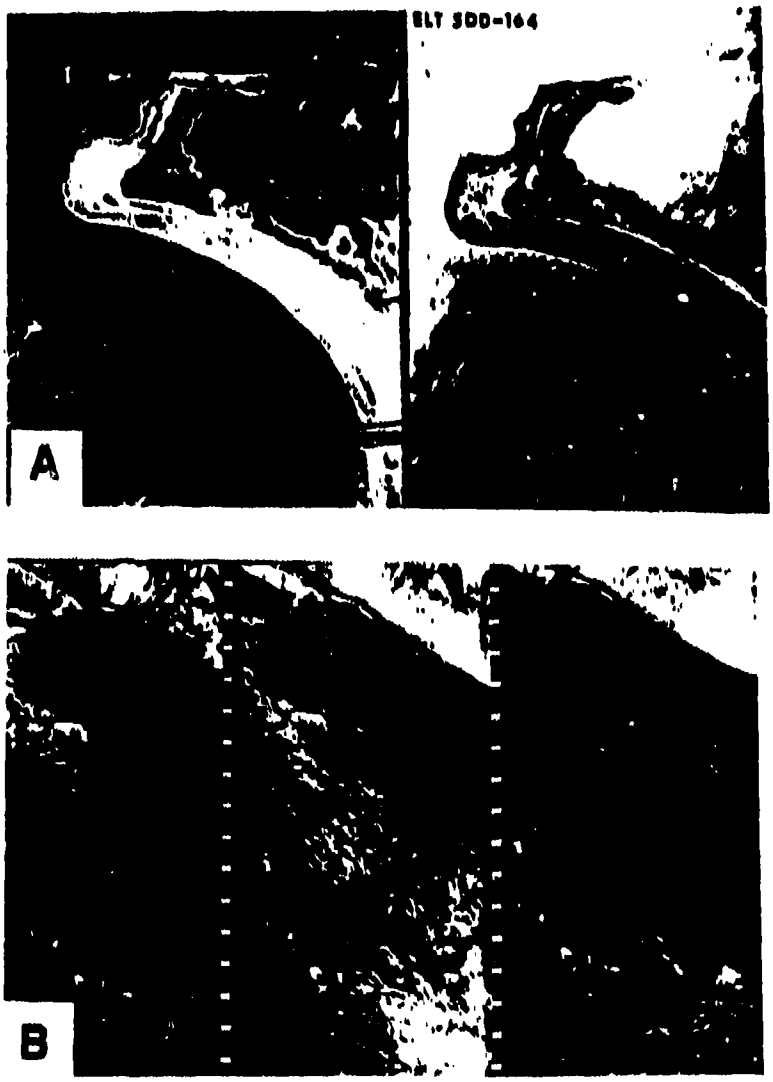

Figure 13. Influence of surface structure on reflectance. The upper set is of Puerto Rico. The right image (from frame 164) has a look angle towards the sun, whereas the left (from frame 169), which overlaps the same area and was taken some minutes later while flying the next line, has a look angle away from the sun. Because of these different viewing angles, there are changes in tone contrast. Without the sun glint there is an improvement in shallow bottom detail in the bay and in shoal areas (Arrow 1), loss of a small pond (Arrow 2), and loss of the wave pattern. The lower set of sequential air photos is of lava flows on the island of Hawaii. There was enough overlap to record the same piece of ground in each image, but from a different look angle in relation to the sun. A reversal of tones is evident throughout.

169. Exposed beach in the bay area of image 164 is easily identified, but not so in image 169. Part "B" of Fig. 13 shows tone changes associated with lava flows in a caldera on the island of Hawaii. The caldera edge is at the bottom of the images. The three frames are from sequential air photos showing the same scene as viewed towards the sun, directly above the feature, and away from the sun. Note the reversal of tones throughout the area of the flows.

2.3 EMITTANCE

Radiation absorbed by a material leads to other effects. For one, absorbed photons increase the internal energy, or temperature, of the material, which, in turn, increases the quantity and alters the wavelength distribution of the thermally emitted radiation, both infrared and microwave. This is the most common outcome of absorption, and is the basis for thermal, or passive, remote sensing in either the infrared or the microwave domain. During daylight hours, absorbed sunlight heats the terrain. During the night, the terrain cools by radiating into space, and would continue to cool except that the sun comes up and renews the heating cycle.

At temperatures above absolute zero (0° K or -273° C), all matter emits electromagnetic energy. If hot enough, such as a hot stovepipe, a tungsten light bulb, or the sun, the object emits enough energy to affect the eye, or a photographic emulsion. At normal earth surface temperatures (-50° to +50° C), however, the amount of energy emitted is below the threshold level of either a photographic emulsion, or the eye. To detect such low levels of photons, special materials are used that are not only sensitive to infrared radiation, but which have some property, such as electrical resistance, that changes rapidly and significantly with variations in intensity of the incoming radiation. This signal is amplified, displayed on a cathode ray tube, and recorded on magnetic tape, or on photographic emulsions via a modulated glow tube, or other device. By convention, except for meteorological satellites, the images are printed so that light tones represent warmer surfaces, and dark tones represent cooler surfaces.

The amount of energy emitted from a surface, and its wavelength distribution, depend on temperature. The amount is equal to the fourth power of the absolute temperature multiplied by the emissivity. For a given temperature, the wavelength distribution curve will have a maximum intensity at a specific wavelength known as lambda sub-max (λ_{max}). Regardless of temperature, 25 percent of the energy will be emitted at wavelengths shorter than λ_{max}, and 75 percent at longer wavelengths. As the temperature gets higher, λ_{max} shifts to shorter wavelengths, e.g., at -150° C it is about 23.2 μm, at 0° C it is about 10.5 μm, and at 100° C it is about 7.7 μm. At the sun's temperature, λ_{max} is about 480 nm. Also, as the temperature gets higher, the short wavelength edge of the distribution curve includes higher energy levels, i.e., it goes to shorter wavelengths, and the area under the curve (total energy emitted) gets rapidly larger. Keeping emissivity constant, a warmer body will emit more energy at all wavelengths than will a cooler body, and will incorporate a short wavelength increment denied the cooler material. Thermal infrared techniques are associated with two wavelength regions for which the atmosphere is transparent, i.e., atmospheric windows. These are the 3.5-5.5 and 8-14 μm bands. For normal earth surface temperatures, i.e., -50° to +50° C, the wavelength of peak emission is in the 8-14 μm band. About 40 percent of the energy is emitted in this band, and about 3 percent in the 3-5.5 μm band. For mapping thermal variations in the terrain the 8-14 μm band is the preferred choice. Above 250° C, the wavelength of peak emission enters the 3-5.5 μm band. For detecting hot targets, this band is the preferred choice. The signal/noise ratio, or the target/background contrast is much greater here. Emissivity, which is wavelength dependent, denotes how good an absorber or emitter, a material is. Molecules emit energy only at those wavelengths they can absorb. A perfect absorber, or emitter, has an emissivity of 1. A material that absorbs 50 percent of the incoming radiation, and reflects 50 percent, has an emissivity of 0.5. So, if two materials have the same physical temperature, but differ in their emissivities, the one with the higher emissivity will emit more energy than the one with the lower, and will be brighter in the image. Many earth materials have emissivities in the 0.7-0.9 range, which means they are fairly good absorbers. This being so, radiation emanating from them is pretty much of surface and near-surface origin. Radiation from molecules at depth is absorbed by molecules above, reradiated and absorbed by the next layer, and passed along until there are

molecules that can radiate into space. For infrared, the depth of the layer that radiates into space is a fraction of a millimeter. The effective depth of this layer increases with longer wavelengths, being perhaps 2.5 cm in the microwave L-band (23 cm).

This layer is an interface between the material below, and the atmosphere above, and is readily influenced by events on both sides. Below, energy transfer is associated with conduction and, in some cases, diffusion. Above, atmospheric variables take over. These can quickly, and radically, alter the radiation characteristics of the surfaces—eliminating, subduing, or increasing thermal contrast. Thus, thermal contrast is influenced by a variety of diurnal and seasonal variations in climatic and meteorological factors, such as wind, atmospheric pressure, dew, rain, humidity, incoming space radiation, etc. Wind can override subsurface conductive events and imprint its own temperature regime, which can create confusing thermal patterns in the form of wind shadows—i.e., surfaces in the lee can be much warmer, or cooler, than surfaces exposed to the wind.

Objects sticking up into the air take on the temperature characteristics of the air. At nighttime, when the air is warmer than the ground, which is cooling by radiation loss, these objects will appear as hot spots—giving signals similar to vehicles with their engines running, as in Fig. 14. As the night progresses, the air layer, cooled by contact with the cooler ground, becomes thicker, and sequentially cools taller and taller objects that project up into it. By late night the hot spots disappear, except for the tops of the tallest trees, or for natural or artificially maintained heat sources.

Also, cooler air is more dense, and, being more dense, it flows downslope to settle in the lows, which show as darker tones in the thermal imagery. Darker tones in the lows can also be caused by moist soil, which has a higher thermal conductivity than dry soil, and can lose heat faster. As a result, cool air drainage into the lows is sometimes mistaken for moist soils.

For detection of voids in the terrain, such as caves, tunnels, crevasses in an icecap, or buried installations, atmospheric pressure changes are critical. First, the interior temperatures are usually fairly constant, and are warmer or cooler than the ground surfaces at some time of the day. Also, infrared cannot penetrate the overburden to reveal the presence of the void. The best time to fly is when the void is exhaling, and the outpouring flow of warm air through various openings brings the temperature of the surrounds to above ambient, and they become detectable—i.e., one detects the openings, not the void. Such an outpouring can occur only when the atmospheric pressure is less than the air pressure in the void. Thus, the time to fly is on a descending pressure front (Rinker, 1975a). Figure 15 shows examples of this.

2.4 LUMINESCENCE

Another effect of photon absorption is luminescence. There are materials that can absorb photons of one frequency and emit photons of a lower frequency, i.e., lower energy, without any significant increase in temperature. These materials are said to be luminescent. An example is the emission of visible light from minerals when they are illuminated with "black" light, or ultraviolet radiation. Luminescence is an emission of radiation due to electronic transitions, and there are two kinds—fluorescence, which occurs from an excited single state, and phosphorescence, which results from an excited triple state. A distinction can also be made on the basis of time—i.e., how long does the light last after the excitation energy is turned off? This is called the decay time. In fluorescence, the decay time is very short, ranging from 10^{-9} to 10^{-3} seconds. For example, the fluorescence decay time of rhodamine B in water is about 2.5 nanoseconds (ns). In phosphorescence, the decay time is longer—sometimes much longer. Calcium sulphide, for example, can continue to glow for several hours after the excitation illumination is turned off.

Luminescent techniques require an energy source to excite, or raise the electrons to higher energy levels, and darkness in order to detect the luminesced photons. The sun meets both of these needs—as does the nighttime use of lasers. The sun does not emit a continuous spectrum, i.e., energy at all wavelengths, or frequencies. Although such is generated in the hot core, electronic absorption by elements and ionized atoms

IR THERMAL IMAGERY, PbTe (3.5 MICRON FILTER) - USA SIPRE, HOUGHTON, MI

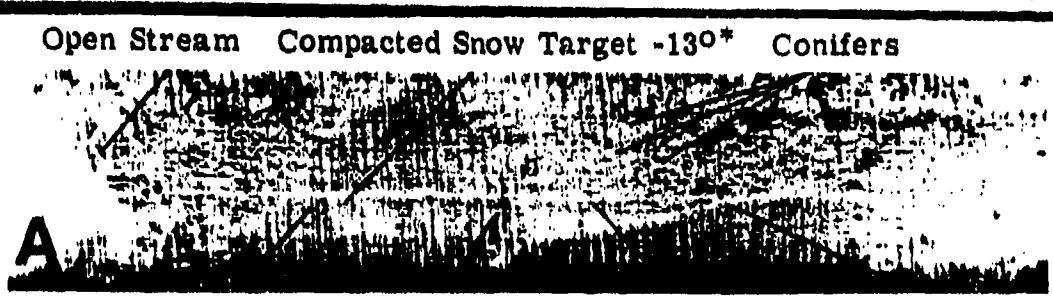

Adjacent Snow -14° W-6 (roof) -3° W-16 (engine on) Conifer

2031 HRS., 9 DEC. 1959. Air temp., -5°C. Surface wind, 6mph.

Adjacent Snow -22° W-16 +16° Trail -15° Crusted Snow -17°

2036 HRS., 10 DEC. 1959. Air temp., -7°C. Surface wind, 0-1 mph.

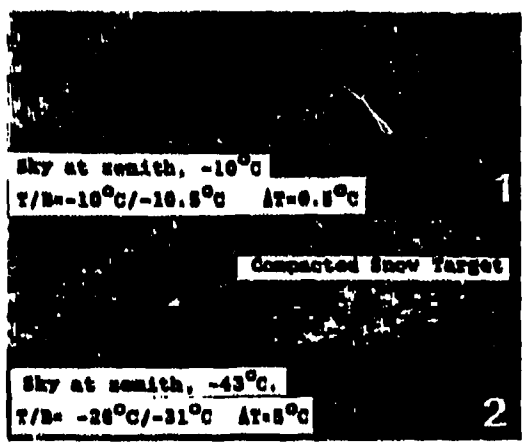

D1: 2016 hrs., 2/14/60, clear.
D2: 2345 hrs., 2/13/60, thin overcast.

Figure 14. Thermal IR images over the USA Snow, Ice, and Permafrost Research Establishment (SIPRE) field site at Houghton, MI. Modified Michigan AN/AAR-9 scanner with a lead telluride, 3.5 micron filter. A and B show the potential for confusion between vehicles and isolated conifers in the mixed hardwood forest (Morgan et al., 1962). Image A also shows influence of surface wind on thermal contrast (1° C) between the compacted snow target and adjacent undisturbed snow. Image B had zero wind, and a stronger thermal contrast (7° C). Image C is from the same general area during the 1959-1960 winter flights (date/time details lost). The isolated light-tone spots are conifers in the mixed hardwood forest. Images D1 and D2 illustrate the influence of incoming long wave radiation on IR thermal contrast (Rinker, 1962). D1 (2016 hrs., 14 Feb 1960) had a target/background Delta T of 0.5° C, and D2 (2345 hrs., 13 Feb 1960) had a Delta T of 5° C for the same target/background. For D1: air temperature, -9° C; compacted snow, -10° C; undisturbed snow, -10.5° C; sky at zenith, -10° C. For D2: air temperature, -19° C; compacted snow, -26° C; undisturbed snow, -31° C; sky at zenith, -43° C.

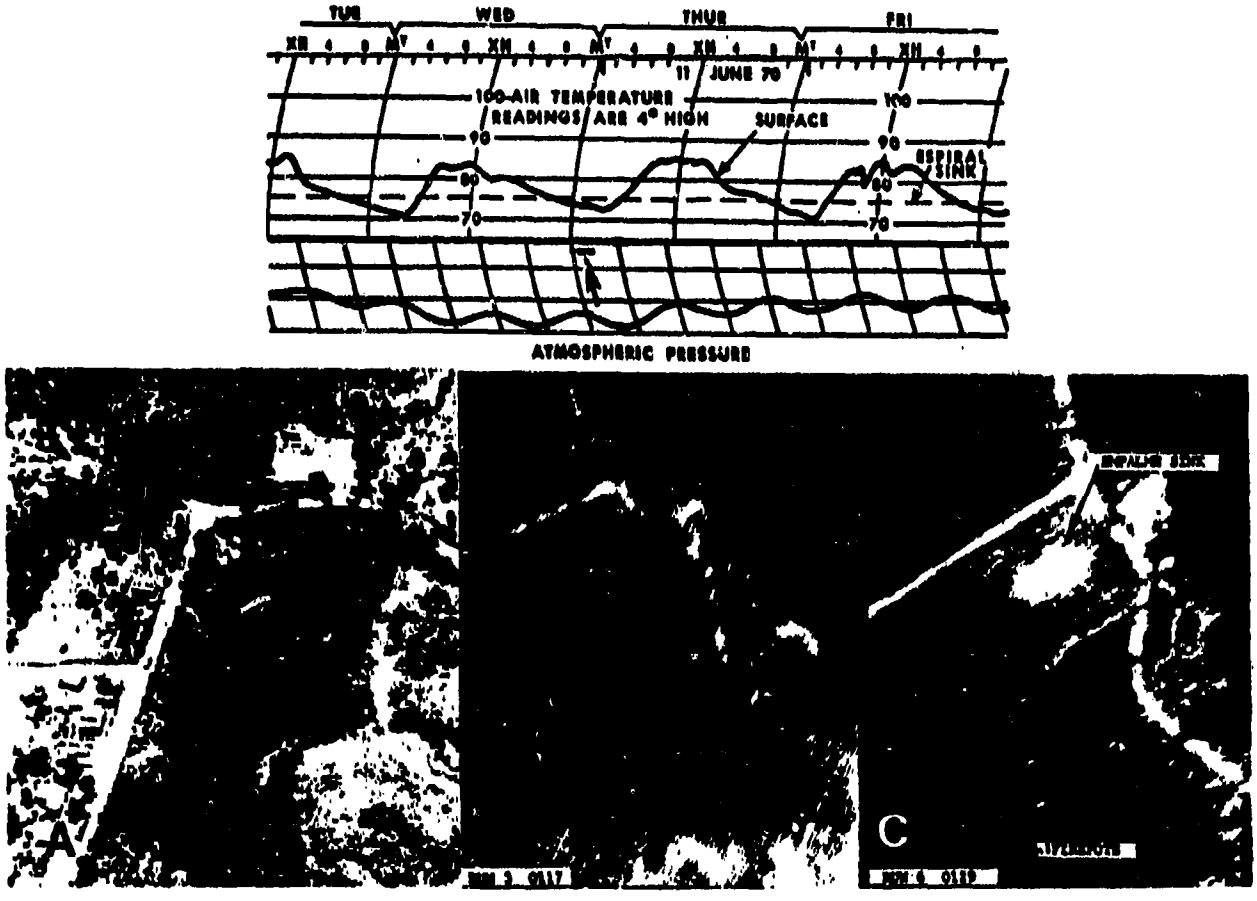

Figure 15. Influence of atmospheric pressure changes on void detection. Images of the Camuy Cave area in Puerto Rico. The top graph shows temperature traces for the surface and the interior of a sinkhole. The bottom graph is a barometric trace. The arrow indicates the time frame of the IR thermal flights, which is during a decreasing pressure phase. Photo A is an aerial oblique of Empalme sink, one of the sinkhole connections in the cave system. Thermal images B and C are of Empalme sink. Image B (Run 3, 0117 hrs) is at the beginning of the exhaling cycle, and the sinkhole is not discernable. Image C (Run 6, 0129 hrs) is later in the pressure drop and Empalme sink has developed a strong signal (Rinker, 1975a).

in the cooler outer envelope greatly reduces the intensities of many of the frequencies. When the sun is examined with a good spectroscope, one finds that there are gaps—many gaps—wherein energy is greatly reduced, or absent. These gaps of darkness are narrow in bandwidth, so narrow they are called lines—specifically, Fraunhofer lines in honor of their discoverer. The spectral bandwidths of these lines are measured in Angstrom Units, frequently in fractions of an Angstrom Unit. The ultraviolet, visible, and near infrared portions of the solar spectrum contain over 30,000 Fraunhofer lines, or lines of darkness. These lines provide the darkness needed for detection of the luminescence, and the sun's radiation provides the excitation energy on the short wavelength side of the lines.

A sensor system that can look at both the sun and the earth's surface with detectors sensitive to energy in these dark lines can detect the presence of luminesced photons from the earth's surface, or target. If, from the target, it detects a certain intensity in a dark line band, it cannot be reflected solar energy because such is not coming from the sun. The fill-in must, therefore, be due to luminesced photons from the target. Such is the function of the Fraunhofer Line Discriminator (FLD) previously mentioned (Hemphill and Settle, 1981, and Hemphill et al., 1989).

Such things as temperature and pH can alter the characteristics of the luminesced photons. Some materials that are under constant, or steady-state illumination, give a different luminescence signal after an hour or two, than they do to an instant measurement immediately after excitation. These changes show as an increase in intensity at longer wavelengths of emission and a decrease of the shorter wavelength components. In fact, some molecules show little luminescence when first illuminated, but develop an intense emission after steady-state illumination. These characteristics are usually associated with liquids and are indicative of changes caused by chemical reactions. Also, the recorded emission spectrum can be distorted in the short wavelength region by self-absorption within the solution. Whether or not these factors are of concern to remote sensing of earth surface and targeting materials is moot. Some materials, such as vegetation, have a near surface liquid component, and chemical reactions are taking place—e.g., photosynthesis. Furthermore, these surfaces are receiving steady state illumination from the sun for hours. In laboratory measurements, the illumination, i.e., the excitation mode, is of short duration. Another characteristic of luminescence is that for any specific wavelength of excitation, there is an emission spectra that can take place over a fairly broad wavelength band, and the decay times of the longer wavelengths can be considerably longer than those of the shorter wavelengths. The total is still a very short time. In laboratory experiments, decay time spectra have shown links to material types and conditions. Whether or not such has application in remote sensing remains to be determined. Abu-Zeid et al. (1987), and Quinn et al. (1988) studied decay characteristics of crude oil. From the standpoint of luminescence in general, Stoertz (1972a and b) demonstrated applicability to earth surface and target materials, and Hemphill and Settle (1981) presented a number of applications to earth resources studies.

No matter what sensor is used, there are other factors that influence the signal that one wants to detect. The atmosphere itself can remove energy from the sunlight, as well as add its own component—luminesced induced, thermally induced, or scattered. Sun angle and azimuth in relation to look angle and surface structure can change, and even reverse tonal contrast. Wind and atmospheric pressure changes alter infrared and microwave thermal contrast, and make it possible or impossible to detect some kinds of targets.

3. SENSORS - THE COLLECTORS OF RADIATION

Photographic emulsions were the earliest of the sensors to document landscape scenes, and human activities. By the late 1800s, emulsions went airborne, via balloons and kites, to replace the observer and his notepad for recording terrain characteristics and military items of interest. By WW I, cameras were in airplanes and routinely involved in reconnaissance and targeting. It was recognized early on that if one could sample different wavelengths of radiation, and compare them, one would have a better chance of detecting targets, as well as noting changes in the landscape—a multiband concept, although not called that, was now in place.

The first steps were taken in the late 1940s and the 1950s when the Army, along with other groups, divided the photographic portion of the electromagnetic spectrum into narrower bandpasses by means of various combinations of photographic emulsions and filters. The goal was to improve techniques for detecting targets and mapping conditions such as camouflage, vegetation type, vegetation stress, soil moisture, flood damage, wetland boundaries, to name a few (Rinker, 1975b), and the term multiband photography came into being to describe these efforts. Camouflage Detection Film, i.e., Ektachrome Infrared film, is one example of a successful film/filter combination, or multiband approach which later passed into the digital domain of Landsat as the False Color Composite. The bandpasses were still broad, however, ranging from 60 to 100 nm. Nevertheless, multiband photography was successfully used in various forms of targeting, and change detection.

Next came the Landsat MSS, which recorded reflected sunlight in four broad bands—two in the visible, each of which is 100 nm wide, and two in the infrared, with one being 100 nm wide and the other 1.1 μm. This was followed by the Landsat TM with six bands in the reflected solar region, and one in the thermal infrared, with the narrowest band being 60 nm for band 3. Spectral variations in the terrain within any of these bands are averaged out to arrive at a digital number (DN) representing the brightness for the whole band.

Extensions of the multispectral concept into the thermal infrared region of the spectrum include the Advanced Very High Resolution Radiometer (AVHRR), and the airborne Thermal Infrared Mapping System (TIMS) developed by Daedalus Enterprises, Inc.

In the early 1980s, a system came forth that greatly altered the existing concepts of multispectral remote sensing with reflected solar energy. This was the Airborne Imaging Spectrometer (AIS) developed by the Jet Propulsion Laboratory (JPL). Details of this system and some of the application results can be found in reports by LaBaw (1983), Vane and Goetz (1985), and Vane (1987). The AIS records reflected solar energy in some 128 channels, or images, within the 1.2-2.4 μm region of the spectrum and with a spectral bandwidth for each channel of less than 10 nm. The AIS evolved into the AVIRIS with some 220 raw data channels, or images, within the 0.4-2.45 μm portion of the spectrum. Resampling gives 210 spectral bands of radiometrically calibrated data. The IFOV is 1 milliradian, or about 10 m at operational altitude. Each image is a record of the intensity of reflected sunlight within a spectral bandwidth of less than 10 nm. After calibrations and corrections have been made, the intensity values of the 210 channels, for any given picture element (pixel), can be called up and sequentially displayed along the wavelength axis, as a spectrophotometric trace, i.e., radiometric intensity versus wavelength. Because of the narrowness of the bands, as well as their multiplicity, these systems are called hyperspectral, to differentiate them from the broad band systems, e.g., MSS, TM, SPOT, etc. Systems are also being developed that can operate in even narrower bands, i.e., the sub-nanometer range, for working with gaseous emissions and absorptions. These are called ultraspectral systems.

Since the advent of the AIS and the AVIRIS, other airborne narrow bandpass systems have been developed, and plans laid for satellite follow-ons. Details of these earlier concepts can be found in a Proceedings Issue of the Society of Photo-Optical Instrumentation Engineers (Vane, 1987b). Current capabilities and system characteristics will be covered in Tutorial IV.

Figure 16 portrays the image cube concept. The stack of images, seven for Landsat TM, and 210 in the case of AVIRIS, forms an image cube. The X and Y axes relate to ground, or pixel location, and the third axis to wavelength. Because of interest in all natural and man-made surfaces, and the need to work with diverse remote sensor data, the wavelength axis of the image cube should extend from the ultraviolet, through the reflected solar, thermal infrared, and microwave regions, out to at least L-band radar at about 23.5 cm wavelength, as shown in the figure. Moreover, we must be concerned with all photons—reflected, emitted, and luminesced—and be able to move back and forth along the image cube axis, incorporating, evaluating, and comparing whatever imagery bands and other data are available, such as Digital Terrain Elevation Data (DTED). Once the corrected image files are in the computer, the spectral patterns can be evaluated by placing the cursor on the site of interest and bringing up a record of the DN values of each of the involved channels. As a minimum, these data should be displayable as line spectra, intensity versus wavelength spectra, and, in the case of luminescence, as three-dimensional spectra (intensity, excitation, emittance), and as contour plots. The spectra can be evaluated in a number of ways, either directly, or by comparison to a computer library of spectral data bases and models. This will be covered in Tutorial III.

Because the atmosphere absorbs many wavelength components of the incoming sunlight, as well as of the reflected energy *en route* to the sensor, corrections are needed for many targets. If one is interested in vegetation, this involves the depths and shapes of water absorption bands. Because water vapor is a component of the atmosphere, the analyst does not know how much of the depth and shape of those water bands is due to atmospheric absorption, and how much is due to vegetation absorption. If corrections can be made to remove the atmospheric component via available models such as LowTran, then the residuum can be attributed to plant water. The notion has been expressed that 220 bands is overload, and that such a multiplicity of bands will lead to data constipation in the collection system, the transmission system, and the data reduction and manipulation systems; and, to ease this, unneeded bands should be eliminated from the collection system. But, which ones can be eliminated—which ones are unneeded? For a narrowly defined goal, the question is easier to answer. For targeting minerals, the geologist can get by with perhaps 30 bands. For determining crop quantity and quality, the agriculturalists can get by with perhaps 20 bands, only a portion of which overlap the geologists' needs. With the combined interests in terrain, targeting, and intelligence, there is need for

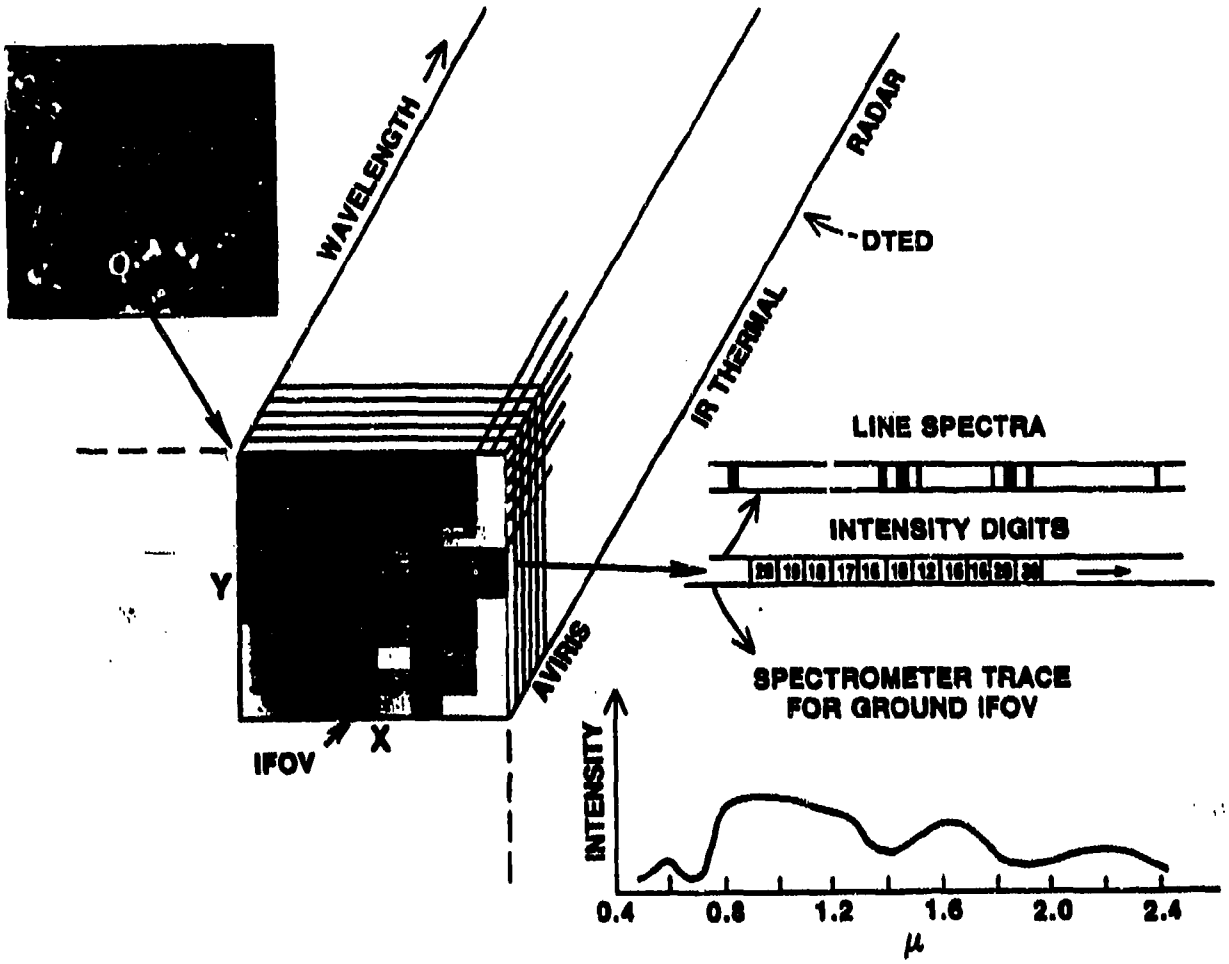

Figure 16. Image cube schematic. On the image cube, X and Y indicate ground coordinates, and the third axis is wavelength. This axis should extend from the ultraviolet out to the lowest frequency radar, and be able to incorporate other data such as Digital Terrain Elevation Data (DTED). For any pixel marked by the cursor, one can sequentially display the intensity values for the bands involved, e.g., MSS, TM, TIMS, AVIRIS, etc., as a line display or as a radiance plot of intensity versus wavelength, either in terms of radiance values, or as normalized values as in this graph. These can be compared to computer stored spectral data bases to arrive at probable identities. Or, the scene can be searched for all locations that are a spectral match, within some variance range, for a given spectral signature.

information about identities, conditions, and properties associated with vegetation, soils, rocks, minerals, water bodies, and cultural objects including camouflage. Perhaps reductions can be made—perhaps there are bands that have no use for anybody—but, it is too early for positive declaration.

4. SPECTRAL DATA - INFLUENCING FACTORS - RESEARCH ISSUES

Spectral data from imaging spectrometers can be evaluated on the basis of: shape of the overall curve, or portions of it; intensity differences at any selected wavelength range; wavelength location of absorption bands; and, depth and shape of absorption bands. To link these to identities and conditions requires an extensive computer library of field and laboratory measurements of spectral reflectance, luminescence, and emittance throughout the reflected solar, and thermal infrared portions of the spectrum—and the software to make the evaluations and comparisons. Such a library needs excellent documentation, because these measured

values change with a variety of factors. For any given surface, the molecular makeup determines the basic characteristics of absorption, reflectance, luminescence, and emittance. These in turn, are modified by the structure of the surface, and its orientation in relation to the sensor and to the illuminating source. For example, maintaining a constant field of view and a constant viewing angle, while measuring spectral reflectance at different sun angles and elevations, can result in variances of plus or minus 10 percent. With reference to structure, vegetation can have smooth, crenelated, or wrinkled leaf surfaces, and the leaves and stems can have many different sizes and be arranged in many different ways. This means different highlight/shadow ratios, different amounts of transmitted and re-reflected infrared energy through the biomass, and different amounts of radiation reflecting up through the vegetation from the soil surface (Satterwhite and Rinker, 1986).

For a given mineral composition, the spectral signature of a fine textured soil can differ from that of a coarser textured soil. Then, there are the influences of conditions, such as age, growth phase, wet, dry, weathered, lichen covered, etc. New leaves have a different spectral signature than older leaves, wet soil is different than the same soil when dry, a weathered rock surface differs from a fresh surface. In reality, these are different chemical forms, which gets back to the earlier statement that the molecular makeup of a surface establishes the basics of reflectance and absorptance. Keeping the target surface and illumination/sensor angles constant, the spectral signature is further modified by climate, season, and meteorological variations. Changes in incoming short and long wave radiation from space, wind, and atmospheric pressure greatly alter radiometric signatures, as well as target/background contrasts in thermal imagery.

Multiplicity of measurements is necessary because there can be significant variation within any given class of targets, especially in field measurements. For example, one can measure 20 creosote bushes that look alike and are about the same size and age. But, the result will likely be 20 slightly different spectra—perhaps plus or minus 10 percent variance, or more, from a derived norm. The variations are mostly in intensity, not wavelength locations of absorption bands. Although the plants look alike, they are not identical—each has some variance in biomass, structure, openness, etc. These factors alter the characteristics of the energy reflected from the vegetal surfaces, as well as the characteristics of the contributing reflected soil component passing through, or reflected from the canopy.

For current systems and typical target areas, the IFOV (10 m for AVIRIS) encompasses a mixture of surfaces, and the resulting spectral signature is a composite of individual signatures—which presents another problem in relation to digital analysis of spectral data.

The intent is to call up the radiance plot of an area on a hyperspectral image, compare it to a spectral measurements library, and thereby identify the surface material. This can now be done—but, much research remains before the technique can be routinely and successfully applied, regardless of material type, location, or season. Basic to such a procedure is a documented library of field and laboratory spectral reflectance and luminescence measurements, coupled, where possible, to physical and chemical measurements. Issues for research or resolution include:

1. Continued development of image pattern data bases and spectral data bases (reflectance, emittance, luminescence), and an agreed to format.

2. Determination of diagnostic spectral features—pure and mixed spectra (UV, VIS, IR, Microwave).

    a. Feature location (wavelength, frequency).
    b. Intensity levels.
    c. Waveform variations.
    d. Statistical and mathematical analyses.

3. Development of formats for computer search and display of spectral data (radiance, reflectance, luminescence) as line spectra, x/y plots, three-dimensional plots, etc.

4. Atmospheric influences and atmospheric backout.

   a. Test existing theoretical models against empirical data.
   b. Develop and test empirical models.
   c. Are atmospheric corrections needed for all targets?—for all locations?—for all seasons?—for all spectral bands?

5. Can scenes be self-calibrated against known spectral data?

   Image patterns are indicative of surface materials and land cover. If such spectra are in the library, correct against them and apply the correction to the rest of the scene. This would remove atmospheric influence as well.

6. Mixed pixel problem. A sensor's IFOV usually contains some mix of objects, which results in an averaging of the reflectance returns.

   a. How to deconvolute to find component spectra?
   b. There is always a limited mix of components, and the mix varies with location. Can image patterns help determine the most probable mix?
   c. Is deconvolution needed in all cases? Probably not. Many features, e.g., wetlands, bajadas, sand sheets, etc., have typical mixes of components of sand, soil, rock, water, and vegetation that identify them for what they are. The composite spectra, or mixed pixel, might be a preferred indicator for identifying such features, or detecting seasonal changes? Will knowing the mixed pixel signature of a given land cover assist in detecting camouflage?

7. Influence of steady-state solar illumination on luminescence.

8. Relation between Laser induced and solar induced luminescence.

9. Influence of season and conditions on luminescence.

5. SOME RESEARCH RESULTS AND APPLICATIONS

The first example illustrates the need for both reflectance and luminescence spectra. Figure 17A shows the reflectance characteristics of two fabrics, A and C, and of a typical green leaf, curve B. Note the deep water absorption bands at approximately 1.4 and 1.9 μm, which are typical of green turgid vegetation. Fabric C is a reasonable match in the visible and out to about 1100 nm. But, it distorts the 1400 nm water absorption band, misses the 1900 nm band, and would be easy to detect. Fabric A, however, mimics the vegetation throughout the spectral range. Based on the reflectance spectra, it would not be detectable against a vegetal background, and would, in fact, be classified as vegetation. At this point, one needs other spectral information, such as luminescence, or infrared thermal emittance. In Fig. 17B, the luminescence intensities of the fabrics, vegetation, and soils were plotted for the indicated Fraunhofer lines. Fabrics A and C not only have strong signals as compared to soils and vegetation, but have different distributions. Thus, they would be detectable in a milieu of soil and vegetation, and also distinguishable from each other. When bruised, the vegetation showed a strong luminescence that persisted for hours, indicating a possibility for detecting passage of traffic.

Figure 18A shows the reflectances of four differently dyed areas of a fabric. Although they, or their composite signal, would be distinguishable against a background of vegetation, the contrast would not be strong against a mixture of soil and different vegetation types and conditions. On a luminescence basis, however, the fabric has a signal intensity that not only greatly exceeds that of soils and vegetal backgrounds, but occurs at different wavelengths—making detection a certainty if the areal extent is sufficient. These relations are shown

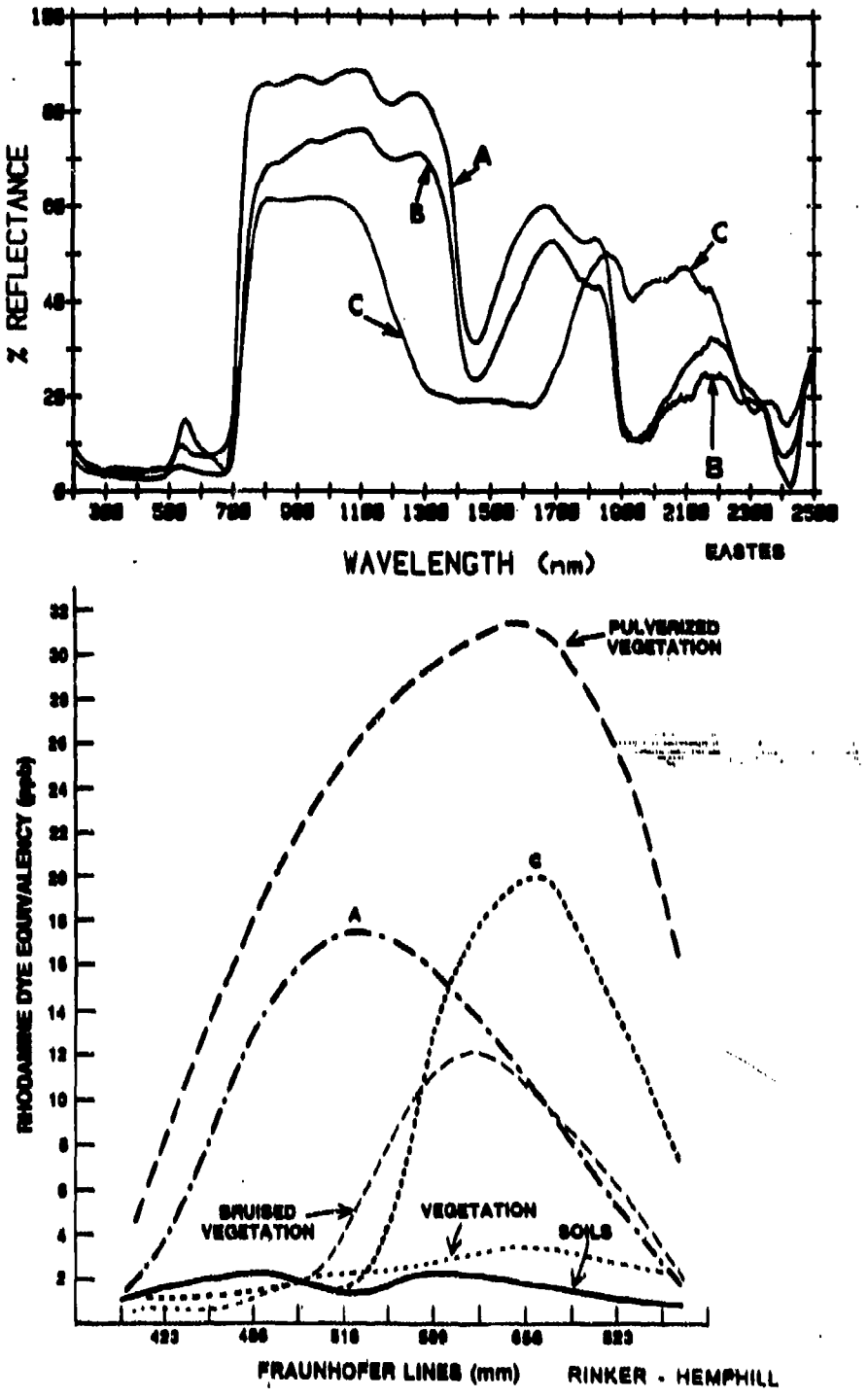

Figure 17. Fabric and vegetation reflectance/luminescence. At the top are spectral reflectances of two fabrics (A and C) and a green leaf (B). The measurements were taken by J.W. Eastes (TEC). Fabric A mimics vegetation, including the water absorption bands, and would be indistinguishable from it. Fabric C is a poor match, and would be easily detected. The lower graph is a plot of luminescence intensity in the Fraunhofer lines of the airborne FLD. These measurements were taken by J.N. Rinker (TEC) and W.R. Hemphill (USGS). Both fabrics show in strong contrast to soils and vegetation (bottom two traces), and also differ significantly from each other. Bruised vegetation gave a strong luminescence signal that persisted for many hours. Pulverized vegetation had even a higher intensity.

in graphs B and C. For airborne detection, the signal threshold is about 1,500 units, and the fabric's luminescence peak is 81,000 units—the "hottest" we had measured to date. In general, the luminescence seldom goes above 12,000 for healthy vegetation. As vegetation senesces, the luminescence increases, but rarely reaches 20,000. The vegetal sample in Fig. 18C, has a peak of 11,000. The iso-intensity contour plot, graph C, shows that the luminescence of the two samples, vegetal and fabric, occurs in different wavelength bands. The original fabric, designed by the U.S. Army Natick Laboratories, matched the luminescence background. What happened? What happened was, the fabric was laundered, and the soap brightener, which luminesces, coupled to the material.

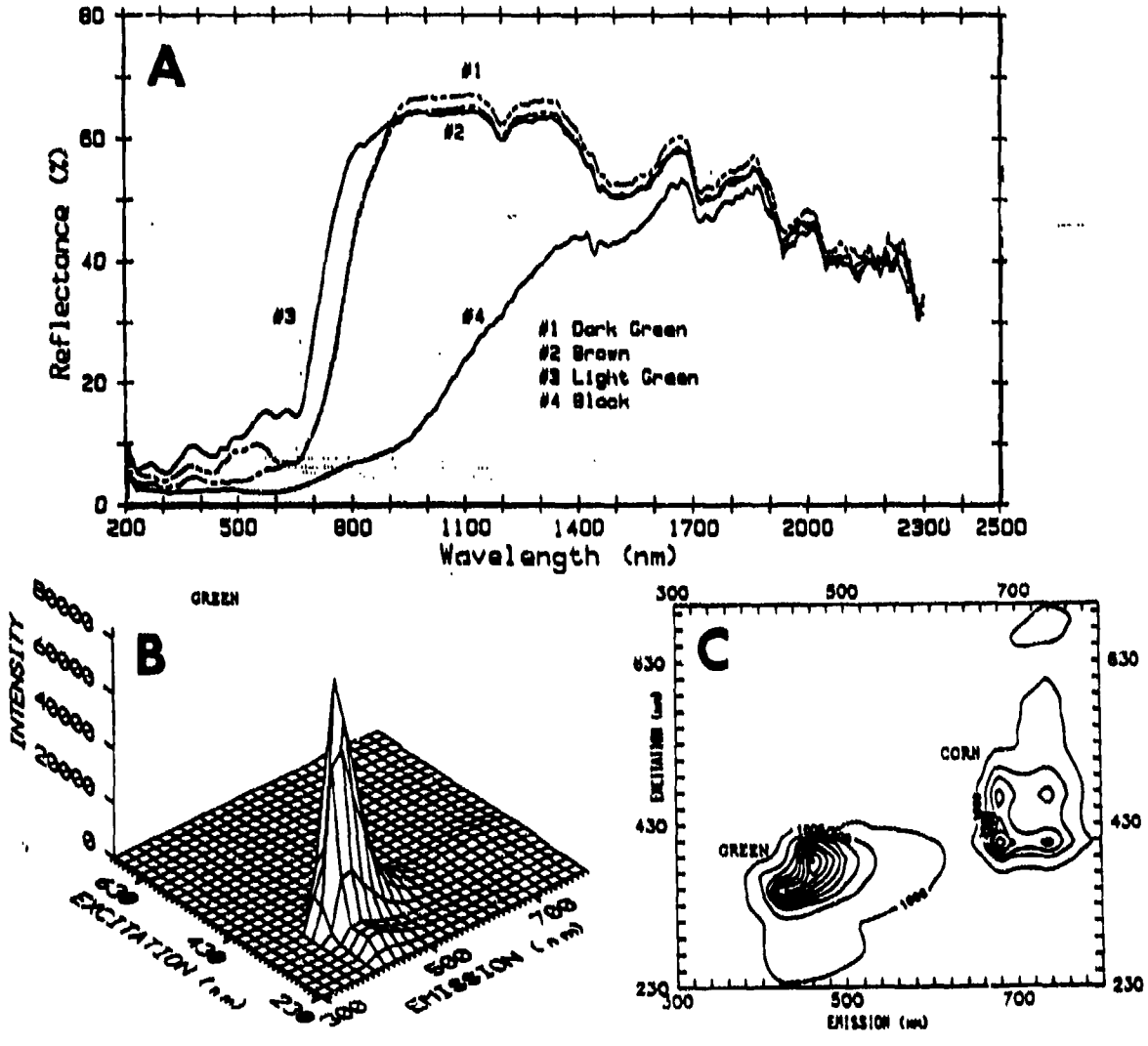

Figure 18. Comparison of fabric reflectance and luminescence. At the top are the reflectance characteristics of four dyed areas of a fabric. Although distinguishable from vegetation, there would not necessarily be a strong contrast, especially if the background provided a mixture of soils and different types and conditions of vegetation. Graph B is a luminescence plot of the green fabric, showing an exceedingly high signal, some 81,000 units. The detection threshold is considered to be 1,500 units. Graph C is an iso-intensity contour plot of the green fabric and of corn, which gives a response typical of healthy herbaceous vegetation. Against the 11,000 intensity units for typical herbaceous vegetation, and the flat response of soils, the fabric with its 81,000 intensity units is easily discernible. It would likely be the brightest object in the scene. This high intensity is attributed to brighteners in the laundry products, as unwashed cloth does not give such a signal. Measurements by M.B. Satterwhite (TEC).

Figure 19 shows some of the differences that take place in vegetal luminescence as a function of drying and of aging. In each example, the upper graph is a three-dimensional display of emission versus excitation, and the lower graph is an iso-contour plot. Figure 19A is typical of healthy, turgid, green leaves, i.e., five distinct luminescence peaks—a group of four with one peak above them. Drying (Plot B) results in a loss of three peaks, reduced intensity in two, and the development of a peak in another area of the plot. Senescence (Plot C) results in the loss of the original five peaks, and the development of two new peaks. Table 3 summarizes these results.

An interesting observation was made by W.R. Hemphill, USGS (personal communication), that when looking out over the terrain with the FLD instrument, there was a strong luminescent signal just above the horizon. It was during the pollen season, and he wondered if the two were connected. Subsequent measurements at TEC confirmed the possibility, as shown in Fig. 20. Implicit in this illustration are a potential application and a potential problem. First, a possible technique for detecting and monitoring airborne pollen loads, i.e., measuring atmospheric quality; and second, a resulting problem—i.e., such an airborne load can reduce contrast, or otherwise interfere with the recording of terrain surface signals.

All materials have spectral reflectance characteristics; but, not all materials have luminescence characteristics. Although we have examined but a portion of what is available, some general statements can be made.

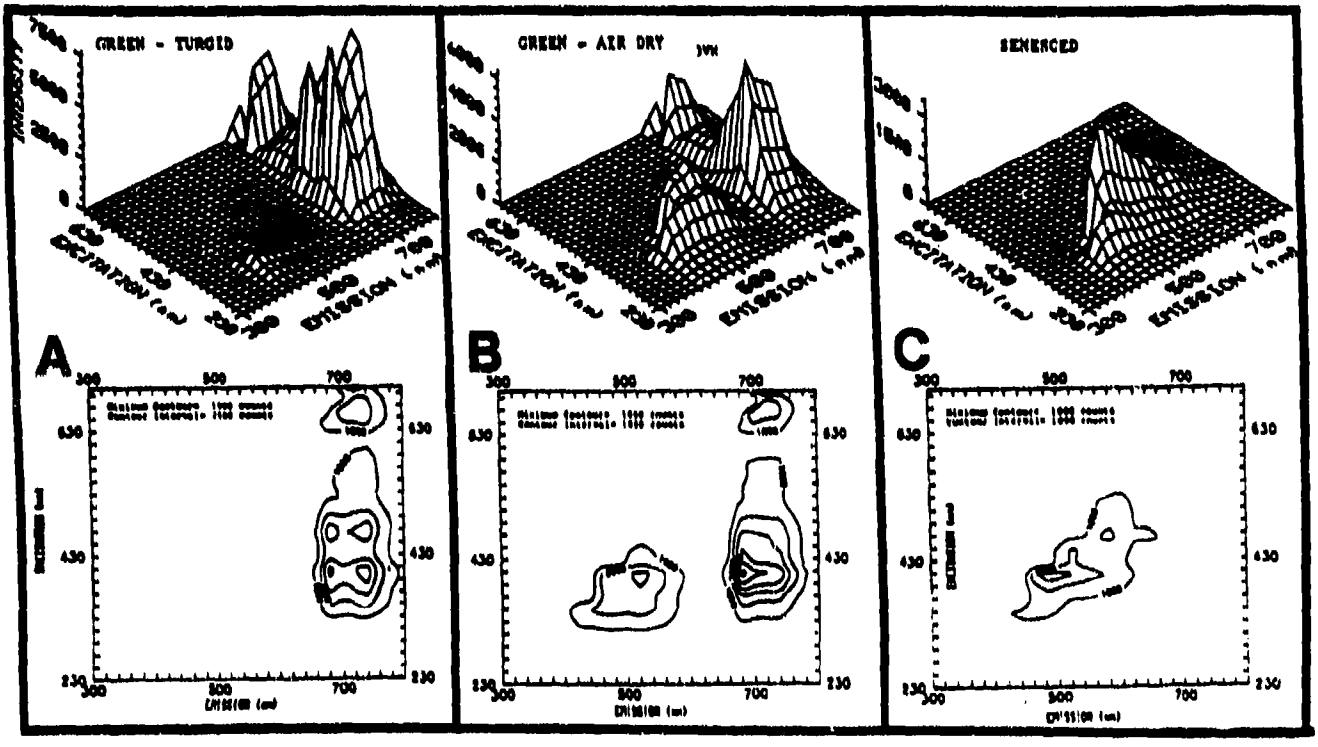

Figure 19. Luminescence characteristics of vegetation. Alteration of vegetal luminescence characteristics as functions of drying and aging. For samples measured so far, these are representative attributes. The upper graphs are three-dimensional displays of excitation wavelength versus emission wavelength versus intensity of the emission signal. The lower graphs are iso-contour plots of the same information. Set A shows the five distinct luminescence peaks—a cluster of four, with a fifth above them. This pattern is characteristic of healthy, turgid, green leaves. With loss of plant water (plot B), three of the lower four peaks fade, and a new peak appears in a different domain of the excitation/emission plot, i.e., in the 430/500 nm wavelength region. Plot C shows the effects of senescence. All of the original peaks are gone, and a new peak has emerged in the vicinity of the peak that developed in response to water stress (Plot B). Measurements by M.B. Satterwhite (TEC).

TABLE 3. LUMINESCENCE BAND CHARACTERISTICS OF VEGETATION

Approximate locations of peak intensities for healthy green vegetation (H), air dried vegetation (AD), and senesced vegetation (S), as taken from the contour plots in Fig. 15. The numbers express the excitation and emission wavelengths in nanometers (nm).

Excitation (nm)	Emission (nm)	H	AD	S
660	730	X	X	
470	680	X		
470	730	X		
400	680	X	X	
400	730	X		
400	500		X	X
470	580			X

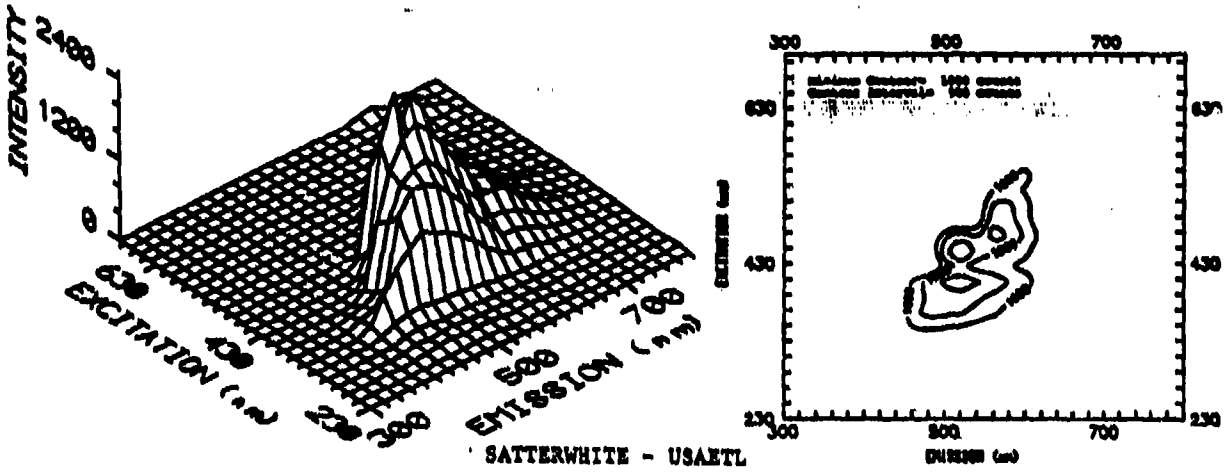

Figure 20. Luminescence characteristics of loblolly pine pollen. Other pollens also luminesce. Pollen of scrub pine is barely detectable, whereas that of cattails has a signal stronger than that of loblolly pollen. Loblolly pollen, however, consists of very small particle sizes and is readily airborne. This suggests a potential technique for monitoring atmospheric components, and also a potential interference problem for collecting terrain data. Measurements by M.B. Satterwhite (TEC).

Soils measured to date do not show useful luminescence. About 75 percent of the vegetal samples and 30 percent of the fabrics have detectable and diagnostic luminescence peaks. For healthy turgid vegetation, the luminescent peaks fall in the wavelength range between 640 and 800 nm. As vegetation dries out, these peaks decrease in intensity and peaks develop in the wavelength region between 400 and 600 nm. Intensity distributions are related to material type and condition, and the peak intensities can be sorted into fairly distinct groups based on emission wavelengths. As shown in Fig. 21, healthy herbaceous vegetation falls into one assemblage, and everything else, e.g., paints, fabrics, pollen, dry vegetation, senesced vegetation, etc., falls in another. So far, with reference to peak emissions, there are three diagnostically useful excitance bands. These are centered at 400, 460, and 660 nm. The important emission bands are centered at approximately 690 and 730 nm.

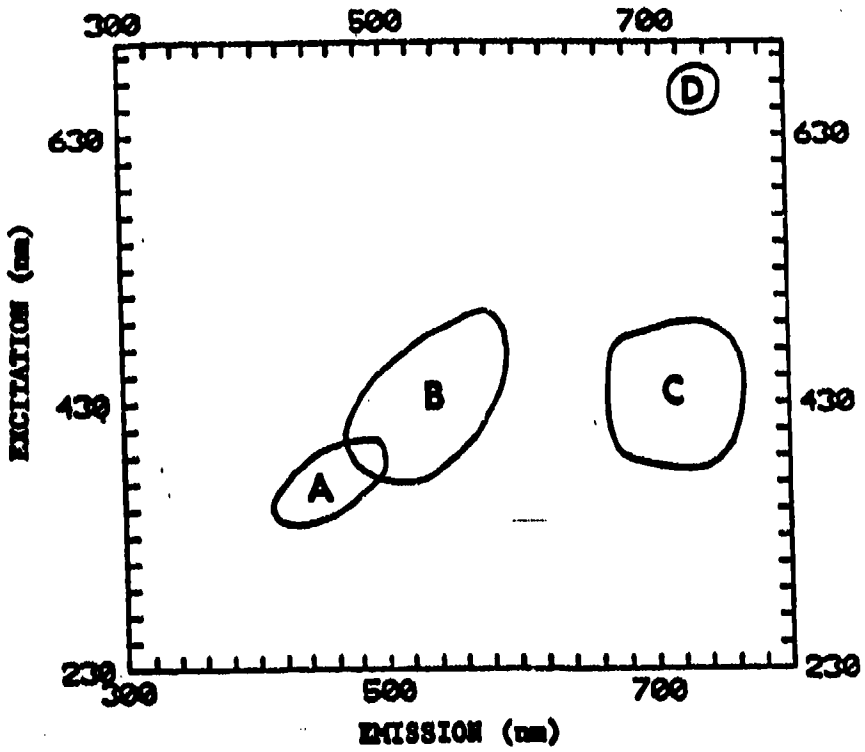

Figure 21. Luminescence classes. On a generalized basis, and for those materials that had usable luminescent peaks, the distributions of the peak intensities fall into the indicated areas. With one exception, so far at least, area A contains the fabrics. Area B, which overlaps A to some extent, contains the peaks of pollen, dry vegetation (pine and herbaceous), and senesced vegetation (pine and herbaceous). Area C contains the peaks of healthy vegetation (pine and herbaceous). Area D has a few secondary peaks associated with herbaceous vegetation. The most useful excitance bands are between 330 and 510 nm. The diagnostic emission peaks fall into two groups, 400-600 nm and 660-760 nm, with the latter containing all the healthy herbaceous samples.

Keep in mind that sensors cannot distinguish between reflected photons and luminesced photons. If sun induced luminesced photons are present, they will be recorded along with the reflected photons, causing a slightly higher DN value or slightly darker gray tone. It is not a large contribution; but, it is a contribution. A spectrometer trace made from a surface illuminated with full-spectrum light, such as the sun, or a halogen lamp, can differ from a record made of a surface illuminated with narrow-band energy at each measurement step. The former situation is characteristic of airborne systems such as AVIRIS, and of field spectrometers, whereas the latter is characteristic of many laboratory instruments, or airborne systems using lasers for illumination, or excitation. For example, luminesced photons from camouflage fabric (refer to Fig. 18) can add to the reflected photon stream to give a slightly higher intensity over the 400-600 nm range. This is shown in Fig. 22, which compares traces recorded from a surface in full illumination and in monochromatic illumination. There can be as much as 8-10 percent absolute difference and 35 percent relative difference. The slight increase in the near infrared region might also be caused by luminescence. It has long been known that vegetation luminesces in the near infrared as the result of the strong absorption at about 645 nm and at about 430 nm (refer to Fig. 19). These added luminesced photons could cause a slight increase in slope steepness of the rapidly increasing reflectance edge just beyond 700 nm, the so-called red edge.

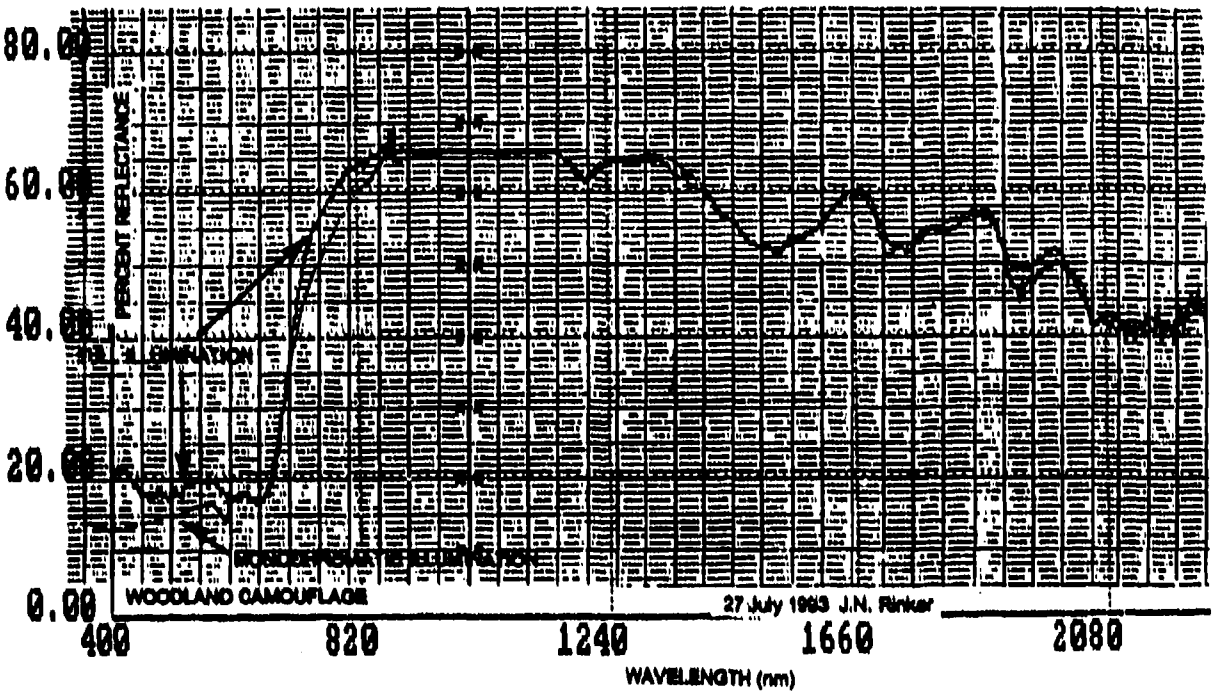

Figure 22. Percent reflectance of Woodland camouflage illuminated with full spectral illumination, or white light (Halogen lamp), and with monochromatic illumination. Full illumination excited the luminescence states, inducing emission of photons at longer wavelengths (refer to Fig. 18). These luminesced photons were incorporated into the stream of reflected photons to cause a slightly higher intensity than was achieved when the sample was illuminated with monochromatic light—most noticeable in the 400-620 nm wavelength region. For example, at 400 nm the sample being illuminated with white light showed a reflectance of about 20 percent. The same surface illuminated with monochromatic light showed about 13 percent reflectance. Once instrumentation differences are eliminated, the most likely cause for the disparity is the added component of luminesced photons. Vegetation also luminesces in the near infrared (refer to Fig. 19), and could easily show an increase in intensity in the 720-850 nm region as a result of luminesced photons. A Perkin Elmer Model 330 spectrometer was used for measurements under monochromatic illumination, and a GER instrument was used for measurements under full illumination.

6. SUMMARY

Remote sensing systems have proved ideal tools for studying earth and atmospheric characteristics, as well as for detecting processes previously unknown. One of the more important tools is the imaging spectrometer, particularly when it covers both the reflected solar band and the thermal infrared bands. An outstanding benefit of an imaging spectrometer is that it provides two domains of information for evaluation—image patterns for terrain information, and spectral patterns for targeting, monitoring, and change detection.

At present, imaging spectrometers provide only monoscopic imagery, so there is a reduction in the quantity and quality of information that can be derived on the basis of image pattern shapes; but, these shapes are present, and they can make significant direct contributions to an analysis, as well as assist in the evaluation of the spectral data. Furthermore, existing routines for combining bands to make color composite images, such as Landsat, or the Coastal Zone Color Scanner (CZCS), can be directly applied to hyperspectral data.

As are many agencies and academic institutions, TEC is collecting field and laboratory spectral measurements of soils, rocks, vegetation, and man-made materials; developing and testing classification and analytical software; and, in cooperation with the USGS group at Flagstaff, AZ, maintaining a series of instrumented test sites that collect around-the-clock measurements of target/background radiation characteristics and concurrent meteorological conditions (Rice and Krusinger, 1985). The resulting data bases (Table 4) support the climatic change program, empirical modeling for target/background contrast prediction and atmospheric backout, assisted target recognition, and digital analysis techniques for hyperspectral imagery.

Basic issues to resolve include: establishing variances within sets; determination of significant spectral bands (statistical, mathematical, empirical) and significant intensity variations; the importance of absorption band slope changes; atmospheric backout in relation to targets, areas, and conditions; self-calibration of imagery from known data base sets; mixed pixel problem; influence of steady state illumination on luminescence; and testing and validation of existing models.

The airborne systems are here, needed spectral data bases exist, and enough hyperspectral image sets (solar reflectance, luminescence, thermal IR) have been evaluated by various interest groups to come to some general conclusions. NASA and JPL have shown the applicability to targeting minerals. USGS, NASA, and USDA have shown applicability to minerals, petroleum, and vegetal characteristics. TEC has shown applicability to military targeting and terrain utilization. The capability exists to render direct assistance to critical national and worldwide problems such as narcotics, disaster evaluation, and global climatic change.

No technique is a panacea, no system does everything, and the hyperspectral, even in its broadest sense, has its limitations; but, from the standpoint of targeting, monitoring, and change detection, the technique has potential beyond any previous remote sensing endeavor. If the system ever achieves stereo imaging capability, we will have the best of both worlds, i.e., stereo image patterns for terrain information, and surface spectral patterns for molecular composition.

TABLE 4. EXISTING DATA BASES IN THE TEC INVENTORY

The temperate data base has nine years of continuous measurements; the subhumid, five years; and the arid, three years. The spectral data bases contain field and laboratory measurements of natural and man-made surfaces, and are collected with an equal or finer spectral resolution than that of the hyperspectral systems. These measurements can be averaged over any selected bandwidth to provide intensity values as they would be in Landsat MSS, TM, TIMS, AVIRIS, etc.

TEC Radiation/Meteorological Data Base - Temperate
TEC/USGS Radiation/Meteorological Data Base - Subhumid
TEC/USGS Radiation/Meteorological Data Base - Arid
TEC Spectral Reflectance Data Base - Solar Radiation (0.4-2.5 μm)[1]
TEC Spectral Reflectance Data Base - Thermal Infrared (2.5-14 μm)[2]
TEC Spectral Luminescence Data Base
TEC/USGS Image Pattern Data Bases - Desert

[1]Satterwhite and Henley (1990)
[2]Eastes (1991)

REFERENCES

Abu-Zeid, M.E., K.S. Bhatia, M.A. Marafi, Y.Y. Makdisi, and M.F. Amer, 1987: Measurements of Fluorescence Decay of Crude Oil: A Potential Technique to Identify Oil Slicks, *Environ. Pollution*, 46, 197-207.

Belcher, D.J., 1943: The Engineering Significance of Soil Patterns. *Proc. 23rd Annual Meeting, Highway Research Board*, Washington, DC.

Eastes, J.W., 1991: Thermal infrared spectra of natural and manmade materials: Implications for remote sensing. U.S. Army Engineer Topographic Laboratories Report, ETL-0587, Fort Belvoir, Virginia 22060-5546.

Fork, R.L., H. Avramopoulos, and J.A. Valdmanis, 1990: Ultrashort Light Pulses. American Scientist, 78, No. 3, 216-223, May-June 1990.

Frost, R.E., J.G. Johnstone, O.W. Mintzer, M. Parvis, P. Mantano, R.D. Miles, and J.R. Shepard, 1953: A Manual on the Airphoto Interpretation of Soils and Rocks for Engineering Purposes. School of Civil Engineering and Engineering Mechanics, Purdue University, West Lafayette, Indiana.

Henley, J.P., 1988: Methods of determining playa surface conditions using remote sensing. *Technical papers of the 1988 ACSM-ASPRS Annual Convention*, Vol. 6, 108-117.

Hemphill, W.R., and M. Settle (Eds.), 1981: Applications of luminescence techniques to Earth resources studies. A Lunar and Planetary Institute Workshop, December 10-12, 1980, LPI Technical Report 81-03, Lunar and Planetary Institute, Houston, Texas.

Hemphill, W.R., J.N. Rinker, A.F. Theisen, and R.H. Nelson, 1989: Potential military applications of passive detection of luminescent materials (U). U.S. Army Engineer Topographic Laboratories Report, ETL-RI-1, Fort Belvoir, Virginia 22060-5546.

Hollas, J.M., 1982: *High Resolution Spectroscopy*, Buttersworth & Company, Ltd., London, Boston.

Hunt, G.R., and J.W. Salisbury, 1970: Visible and Near-Infrared Spectra of Minerals and Rocks: Silicate Minerals. *Modern Geology*, 1, 283-300. First of a series of papers.

Kock, W.E., 1965: *Sound Waves and Light Waves. The fundamentals of Wave Motion*. Anchor Books, Doubleday & Company, Inc., Garden City, New York.

LaBaw, C., 1983: Airborne imaging spectrometer: An advanced concept instrument. *Proc. Soc. of Photographic Instrumentation Engineering*, paper 430.

McCauley, J.F., G.G. Schaber, C.S. Breed, M.J. Grolier, C.V. Haynes, B. Issawi, C. Elachi, and R. Blom, 1982: Subsurface Valleys and Geoarcheology of the Eastern Sahara Revealed by Shuttle Radar. *Science*, 218:4567, 1004-1019.

Morgan, J.E., C.D. Miller, D.C. Parker, D.S. Fisher, J.H. McLerran, J.N. Rinker, and B.L. Hansen, 1962: Operation Cold Deck: A cold regions aerial infrared sensing program (U). U.S. Army Cold Regions Report 104, Hanover, New Hampshire.

Pierce, J.R., 1956: *Electrons, Waves and Messages*. Hanover House, Garden City, New York.

Quinn, M.F., S. Joubian, F. Al-Bhatia, S. Al-Aruri, and O. Alameddine, 1988: Deconvolution Technique for Determining the Intrinsic Fluorescence Decay Lifetimes of Crude Oils, *Applied Spectroscopy*, **42**, 406.

Rice, J.E., and A.E. Krusinger, 1985: A new and extensive thermal contrast data base. *Proc. IRIS Specialty Group on Targets, Background, and Discriminations*, Vol. II, 1-5.

Rinker, J.N., 1962: Aerial detection of snow surface and undersnow targets. *Proc. Army Science Conf.*

Rinker, J.N., 1975a: Airborne infrared thermal detection of caves and crevasses, *Photogrammetric Engineering and Remote Sensing*, **41:11**, 1391-1400.

Rinker, J.N., 1975b: Some technical aspects of film emulsions in relation to the analysis and interpretation of aerial photographs. In *Aerial Reconnaissance for Archaeology*, D.R. Wilson (Ed.). Research Report No. 12, The Council for British Archaeology, 32-46.

Rinker, J.N., and P.A. Corl, 1984: Air photo analysis, photo interpretation logic, and feature extraction. U.S. Army Engineer Topographic Laboratories Report, **ETL-0329**, Fort Belvoir, Virginia 22060-5546.

Rinker, J.N., 1990a: Hyperspectral imagery - What is it? - What can it do? *Proc. Seventh USACE Remote Sensing Symposium*, 7-9 May 1990, Portland, Oregon.

Rinker, J.N., 1990b: Hyperspectral imagery - A new technique for targeting and intelligence. *Proc. Army Science Conf.*, 12-15 June 1990, Durham, North Carolina.

Satterwhite, M.B., and J.P. Henley, 1990: Hyperspectral signatures of vegetation, minerals, soils, rocks, and cultural features: Laboratory and field measurements. U.S. Army Engineer Topographic Laboratories Report, **ETL-0573**, Fort Belvoir, Virginia 22060-5546.

Satterwhite, M.B., and J.N. Rinker, 1986: Time variant reflectance spectra of plant canopies as affected by in-canopy shadow. *Proc. Army Science Conf.*, Vol. IV, 17-19 June 1986, 41-55.

Stoertz, G.F., 1972a: Visible fluorescence of Earth-surface materials and potential applications to remote sensing. **NTIS PB-210-621.**

Stoertz, G.F., 1972b: Feasibility of differentiating target materials by their solar-stimulated fluorescence. **NTIS PB-210-641.**

Vane, G. (Ed.), 1987a: *Proc. of the Third Airborne Imaging Spectrometer Data Analysis Workshop*. Jet Propulsion Laboratory, California Institute of Technology, JPL Publication 87-30.

Vane, G. (Ed.), 1987b: Imaging Spectroscopy II. *Proc. Soc. of Photo-Optical Instrumentation Engineers*, Vol. 834.

Vane, G., and A.F.H. Goetz, 1985: *Proc. Airborne Imaging Spectrometer Data Analysis Workshop*, Jet Propulsion Laboratory, California Institute of Technology, JPL Publication 85-41.